

Electronic Thesis and Dissertation Repository

9-29-2020 1:00 PM

An approach for the in-vivo characterization of brain and heart inflammation in Duchenne Muscular Dystrophy

Joanne Tang, *The University of Western Ontario*

Supervisor: Anazodo, Udunda C., *The University of Western Ontario*

Joint Supervisor: Hoffman, Lisa M., *The University of Western Ontario*

A thesis submitted in partial fulfillment of the requirements for the Master of Science degree in Medical Biophysics

© Joanne Tang 2020

Follow this and additional works at: <https://ir.lib.uwo.ca/etd>



Part of the [Animals Commons](#), [Cardiovascular Diseases Commons](#), [Cellular and Molecular Physiology Commons](#), [Immunopathology Commons](#), [Investigative Techniques Commons](#), [Laboratory and Basic Science Research Commons](#), [Medical Biotechnology Commons](#), [Musculoskeletal Diseases Commons](#), and the [Nervous System Diseases Commons](#)

Recommended Citation

Tang, Joanne, "An approach for the in-vivo characterization of brain and heart inflammation in Duchenne Muscular Dystrophy" (2020). *Electronic Thesis and Dissertation Repository*. 7394.
<https://ir.lib.uwo.ca/etd/7394>

This Dissertation/Thesis is brought to you for free and open access by Scholarship@Western. It has been accepted for inclusion in Electronic Thesis and Dissertation Repository by an authorized administrator of Scholarship@Western. For more information, please contact wlsadmin@uwo.ca.

Abstract

Duchenne muscular dystrophy (DMD) is a neuromuscular disorder caused by dystrophin loss—notably within muscles and CNS neurons. DMD presents as cognitive weakness, progressive skeletal and cardiac muscle degeneration until pre-mature death from cardiac or respiratory failure. Innovative therapies improved life expectancy, but this is accompanied by increased late-onset heart failure and emergent cognitive degeneration. Thus, there is an increasing need to both better understand and track disease pathophysiology in the dystrophic heart and brain prior to onset of severe degenerative symptoms. Chronic inflammation is strongly associated with skeletal and cardiac muscle degeneration, however chronic neuroinflammation's role is largely unknown in DMD despite being prevalent in other neurodegenerative diseases. Considering the well-known consequences of unchecked chronic inflammation, inflammation's contribution towards multi-organ degeneration must be explored. Thus, this study explored inflammatory marker translocator protein positron emission tomography (TSPO-PET) to evaluate immune cell infiltration within the hearts and brains of DMD murine models. Four DMD and six healthy mice underwent whole-body PET imaging using the TSPO radiotracer [¹⁸F]FEPPA. Confirmatory TSPO-immunofluorescence staining of cardiac and neural tissues were also conducted. Our results indicated that DMD mice showed significant elevations in heart and brain [¹⁸F]FEPPA activity, which correlated with increased *ex-vivo* fluorescence intensity. In summary, this study suggests cardiac and neuroinflammation presence in DMD and highlights TSPO-PET's utility as a tool for *in-vivo* assessment of inflammation in several organs simultaneously within DMD.

Keywords

Duchenne muscular dystrophy, [¹⁸F]FEPPA, positron emission tomography, neuroinflammation, cardiac inflammation, *mdx:utrn*(+/-)

Summary for Lay Audience

Duchenne muscular dystrophy is characterized by progressive skeletal and heart weakness, and cognitive impairment. Current therapies have increased patient longevity, revealing the emergence of heart and brain degenerative symptoms at the later stages of the disease. Thus, there is a need to better assess, understand, and track the potential sources of multi-organ dysfunction in DMD. Inflammation is thought to be a prime contributor to these dysfunctions because it is widespread in both the DMD patient's muscle and blood. However, not much is known about inflammation in the brain of DMD subjects. This work addresses this gap in knowledge through the assessment of inflammation in the brains and hearts of DMD mice using live animal imaging and tissue measurements of [¹⁸F]FEPPA, a radiotracer that accumulates in inflammatory cells. We found higher [¹⁸F]FEPPA in the hearts and brains of DMD mice compared to healthy mice. This research demonstrates that imaging using [¹⁸F]FEPPA can be a useful tool to assess inflammation in multiple organs in live mice models of DMD.

Co-Authorship Statement

This thesis is adapted from Tang et al. (submitted to *Neuromuscul. Disord.* August 2020), entitled “*In-vivo* imaging of cardiac and neuroinflammation in Duchenne muscular dystrophy mice: a [¹⁸F]FEPPA study.” This manuscript was co-authored by Joanne M. Tang, Andrew McClennan, Linshan Liu, Jennifer Hadway, Dr. Justin W. Hicks, Dr. John Ronald, Dr. Lisa M. Hoffman, and Dr. Udunna C. Anazodo. J.M. Tang performed the experimental work, methodology design, data analyses, a portion of the animal care and handling, and drafted the manuscript. Andrew McClennan also performed animal care and handling, assisted in the collection/analyses of biodistribution data and in conducting the PET imaging procedure. Linshan Liu assisted in PET data analysis by writing the image-processing Matlab script. Jennifer Hadway assisted in the PET imaging protocol by performing the tail vein catheterization and aiding in general troubleshooting. In addition to providing constructive criticism during thesis/study development, Dr. Justin Hicks aided in PET radiochemistry synthesis and Dr. John Ronald was consulted for the immunostaining results. Dr. Lisa Hoffman and Dr. Udunna Anazodo were responsible for the conceptualization/methodology design of this study, in addition to supervision of research activity/planning/execution. Dr. Lisa Hoffman also provided the funding for this study, while Dr. Udunna Anazodo aided in the data collection and analyses. All co-authors listed were also involved in the editing and review of the manuscript.

Acknowledgments

Firstly, I would like to express my utmost thanks to my supervisors, Drs. Udunna Anazodo and Lisa Hoffman for providing me the opportunity to participate in not only this highly multidisciplinary project, but also various supervisory, administrative, and lecturing roles. I am also grateful for your continuous support and guidance; they were intrinsic to both my academic and mental well-being. Lisa, your go-getter attitude and unconcealed passion is contagious—thank you for giving me the strength to keep moving forwards. Udunna, thank you for always keeping your door open (both the physical and Zoom one). I truly respect your work ethic and ambition, and aspire to be of similar caliber one day.

I would also like to thank my advisory committee members Drs. John Ronald and Justin Hicks for their continuous support and constructive criticism. Their feedback was essential in shaping the narrative of this work. My gratitude is also extended to Drs. Jonathan Thiessen, David O’Gorman, and Gedas Cepinskas for both volunteering your time to read this thesis and for being on my qualifying exam committee.

I would like to thank Jennifer Hadway, Lise Desjardins, Haris Smailovic, and Dr. Matthew Fox for their assistance and support during imaging sessions. Each one of them were essential to the study’s successful completion, and I can think of no other people who could have provided better support during the long and obstacle-ridden process.

Additionally, I offer my sincere gratitude to the past and present members of the Anazodo and Hoffman labs: Linshan Liu, Stefan Poirier, Madeline Dacey, Praveen Dassanayake, Andrew McClennan, Yiming Lin, Sarah Hakim, Patrick Murphy, Yasmeen Shweiki, and Niharika Kashyap. They provided me considerable advice and assistance for my project, and made my lab experience far more entertaining and memorable. I would also like to thank the countless volunteers that assisted with lab upkeep. A special thanks to Andrew McClennan for not only his efforts in managing the mice breeding colony, but also for his work during imaging sessions. I also offer my sincere thanks to Linshan Liu for putting up with my continued invasion of her office, and her efforts in aiding in PET image analysis.

I would also wish to acknowledge Caroline O’Neil and the Robarts Research Institute Pathology facility for paraffin-embedding and sectioning our tissues.

Lastly, I would like to extend my sincere thanks to my friends and family for supporting me through this journey. Thank you to especially my dear parents, Bosong Tang and Katherine Zhang, for allowing me to undertake this challenge and providing me the means to see it through. To my father: thank you for imparting to me the importance of hard work, while keeping a sunny disposition. To my mother: thank you for your worry, your love, and your constant support/care. I am also grateful to my friend/roommate of 7 long years for both supporting me throughout this endeavour and acting as my “personalized feedback” companion; thank you and I hope you enjoyed learning about my thesis as much as I did.

I would also like to acknowledge funding support from Children’s Health Research Institute, Western’s Interdisciplinary Development Initiative (IDI) in Stem Cell and Regenerative Medicine studentship, and the Western Graduate Research Scholarship. I also would like to acknowledge the ongoing academic support provided by the Department of Medical Biophysics and the Collaborative Program in Molecular Imaging.

Table of Contents

| | |
|---|----------|
| Abstract | ii |
| Summary for Lay Audience | iii |
| Co-Authorship Statement..... | iv |
| Acknowledgments..... | v |
| Table of Contents | vii |
| List of Figures | x |
| List of Appendices | xi |
| Chapter 1 | 1 |
| 1 Introduction | 1 |
| 1.1 Clinical Symptoms of Duchenne Muscular Dystrophy | 1 |
| 1.1.1 Overview..... | 1 |
| 1.1.2 Life phases | 1 |
| 1.1.3 Clinical Symptoms of the Dystrophic Heart..... | 2 |
| 1.1.4 Clinical Symptoms of the Dystrophic Brain..... | 3 |
| 1.2 Pathophysiology..... | 5 |
| 1.2.1 Overview of Dystrophin | 5 |
| 1.2.2 Dystrophic Cardiac Pathology | 6 |
| 1.2.3 Dystrophic Neural Pathology..... | 9 |
| 1.3 Inflammation Contributes to DMD Cardiac and Neurologic Outcomes | 11 |
| 1.4 Assessments of Inflammation..... | 13 |
| 1.4.1 <i>Ex-vivo</i> Assessments | 13 |
| 1.4.2 <i>In-vivo</i> Assessments..... | 14 |
| 1.5 Inflammatory PET Radiotracers | 16 |

| | | |
|------------------|--|-----------|
| 1.5.1 | Glucose-metabolism Analogue Tracer – FDG | 16 |
| 1.5.2 | Translocator Protein (TSPO) Tracer – FEPPA..... | 17 |
| 1.6 | Pre-clinical Murine Models of DMD..... | 19 |
| 1.7 | Research Outline..... | 20 |
| 1.7.1 | Study Objectives..... | 20 |
| 1.7.2 | Study Hypothesis | 20 |
| 1.8 | References..... | 21 |
| Chapter 2 | | 32 |
| 2 | <i>In-vivo</i> imaging of cardiac and neuroinflammation in Duchenne muscular dystrophy mice: a [¹⁸ F]FEPPA PET study..... | 32 |
| 2.1 | Introduction..... | 32 |
| 2.2 | Materials and Methods..... | 35 |
| 2.2.1 | Study Population..... | 35 |
| 2.2.2 | Small animal PET Imaging Protocol | 35 |
| 2.2.3 | PET Imaging Analysis | 36 |
| 2.2.4 | Biodistribution and Autoradiography | 36 |
| 2.2.5 | Histology..... | 37 |
| 2.2.6 | Statistical Analyses | 38 |
| 2.3 | Results..... | 38 |
| 2.3.1 | Elevation of <i>in-vivo</i> inflammation-targeted radiotracer binding in DMD models..... | 39 |
| 2.3.2 | <i>Ex-vivo</i> TSPO signal indicates heightened cardiac and neuroinflammation in DMD | 40 |
| 2.4 | Discussion..... | 44 |
| 2.5 | Conclusions..... | 51 |
| 2.6 | Acknowledgements..... | 51 |

| | | |
|------------------|---|----|
| 2.7 | References..... | 52 |
| Chapter 3 | | 60 |
| 3 | Conclusions and Future Directions | 60 |
| 3.1 | Study Summary..... | 60 |
| 3.2 | Significance..... | 61 |
| 3.3 | Limitations | 62 |
| 3.4 | Future Directions | 64 |
| 3.5 | Concluding Remarks..... | 65 |
| 3.6 | References..... | 66 |
| | Appendices..... | 70 |
| | Curriculum Vitae | 76 |

List of Figures

| | |
|--|----|
| Figure 1.1. Dystrophin serves as an integral component of the Dystrophin-associated protein complex (DAPC) and links the actin cytoskeleton to extracellular matrix (ECM). | 7 |
| Figure 2.1 [¹⁸ F]FEPPA SUV images of representative 8-10 week wild-type (A, C, E) and age-matched Duchenne muscular dystrophy (B, D, F) mice. | 39 |
| Figure 2.2 Quantified [¹⁸ F]FEPPA activity in hearts (A) and brains (B) of age-matched DMD and wild-type mice. | 40 |
| Figure 2.3 <i>Ex-vivo</i> histology of TSPO-bound microglial and macrophages in DMD and healthy subjects' cardiac (A) and neural tissues (B). | 42 |
| Figure 2.4 Quantified fluorescence immunohistochemical images of microglial and macrophages with TSPO in 8-10 week old DMD and healthy subjects. | 43 |
| Figure 2.5 Correlation of [¹⁸ F]FEPPA uptake with histological TSPO fluorescence intensity. | 43 |

List of Appendices

| | |
|--|----|
| Appendix A: Approval of Animal Protocols | 70 |
| Appendix B: Quantitative autoradiography and Biodistribution of [¹⁸ F]FEPPA-injected 8-10 week old <i>mdx:utr</i> n (+/-) mice..... | 71 |
| Appendix C: Sample sizes for imaging and histologic studies..... | 72 |
| Appendix D: Representative qualitative autoradiography images from [¹⁸ F]FEPPA-injected 8-10 week old <i>mdx:utr</i> n (+/-) mice..... | 73 |
| Appendix E: Copyright Agreement for reproduction of Figure 1.1 | 74 |

List of Abbreviations

| | |
|-------------------------------|---|
| [¹¹C]PK1195 | [¹¹ C]-(<i>R</i>)-(2-chlorophenyl)- <i>N</i> -methyl- <i>N</i> -(1-methylpropyl)-3-isoquinoline-carboxamide |
| [¹⁸F]FEPPA | [¹⁸ F]- <i>N</i> -(2-(2-fluoroethoxy)benzyl)- <i>N</i> -(4-phenoxy pyridin-3-yl)acetamide |
| [¹⁸F]FDG | 2-deoxy-2- ¹⁸ F-fluoro-D-glucose |
| α-SMA | Alpha Smooth Muscle Actin |
| AD | Alzheimer's Dementia |
| AQP4 | Aquaporin-4 |
| BBB | Blood-brain Barrier |
| BSA | Bovine Serum Albumin |
| CACC | Canadian Council on Animal Care |
| CNS | Central Nervous System |
| CRP | C-reactive Protein |
| CT | Computer Tomography |
| DAPC | Dystropin-associated Protein Complex |
| DAPI | 4',6-diamidino-2-phenylindole |
| DMD | Duchenne Muscular Dystrophy |
| DNA | Deoxyribonucleic Acid |
| ECM | Extracellular Matrix |

| | |
|--------------------------------|---|
| FSIQ | Full Scale Intelligence Quotient |
| GABA_A | γ -aminobutyric acid |
| IL-1β | Interleukin-1 β |
| IL-6 | Interleukin-6 |
| IQ | Intelligence Quotient |
| <i>mdx</i> | X Chromosome-Linked Muscular Dystrophy Mouse Model |
| <i>mdx:utrn (+/-)</i> | Dystrophin-Knockout, Utrophin-Heterozygous Muscular Dystrophy Mouse Model |
| MRI | Magnetic Resonance Imaging |
| NF-κB | Nuclear Factor Kappa-Light-Chain-Enhancer of Activated B Cells |
| nNOS | Nitric Oxide Synthase |
| NO | Nitric Oxide |
| PBR | Peripheral Benzodiazepine Receptor |
| PBS | Phosphate Buffered Saline |
| PET | Positron Emission Tomography |
| PFA | Paraformaldehyde |
| PIQ | Performance Intelligence Quotient |
| RF | Radiofrequency |
| ROS | Reactive Oxygen Species |
| SEM | Standard Error of the Mean |

| | |
|-------------------------------|---------------------------------|
| SUV | Standardized Uptake Value |
| TNFα | Tumor Necrosis Factor- α |
| TSPO | Translocator Protein (18kDa) |
| VIQ | Verbal Intelligence Quotient |
| WCST | Wisconsin Card Sorting Test |

Chapter 1

1 Introduction

1.1 Clinical Symptoms of Duchenne Muscular Dystrophy

1.1.1 Overview

Duchenne muscular dystrophy (DMD) is a fatal progressive neuromuscular disorder that affects approximately 1 in 3600 males worldwide, becoming the most commonly inherited pediatric muscle dystrophy. DMD is typically caused by a X-linked recessive mutation in the *DMD* gene, resulting in a higher emergence of pathological symptoms in males than females [1]. However, DMD can also occur as a result of new spontaneous *de novo* mutations, which are thought to occur in approximately one-third of affected boys, while the remaining cases are attributed to the mutation inheritance from their carrier mothers [2,3]. Dystrophin proteins are present in several tissue types, but most notably are found within skeletal muscle, cardiac muscle, neurons within the central nervous system (CNS). In most cases, DMD is characterized by muscle weakness and degeneration, alongside cognitive impairment. These symptoms are often exacerbated by chronic inflammation, and ischemia, often followed by fibrosis until the patient succumbs to an early death from cardiac or respiratory complications [4–6]. Although there is still no cure, recent advancements in experimental therapies have prolonged both ambulation and life expectancy to approximately ages 30-40 [6,7].

1.1.2 Life phases

Infant DMD boys are asymptomatic as the first noticeable symptoms often manifest at 2-5 years, resulting in a late average age of definitive diagnosis at 5 years old. At this time, affected boys typically present lower limb and trunk muscle weakness before substantial muscular deterioration—causing gait problems, calf hypertrophy, Gower’s sign, and other orthopedic complications between the ages of 6-8. By the onset of puberty, the majority of these affected patients will lose a substantial amount of motor function and

become wheelchair-bound—by the age of 10-12—before cardiac and respiratory function begin to deteriorate. The loss of respiratory muscular structures results in decreased pulmonary function, increasing the likelihood of developing respiratory infection and failure by age 20 [1,8,9]. Currently, developments in skeletal muscle treatments (e.g. corticosteroids, gene therapies, etc.) and respiratory care (e.g. use of respiratory assist devices, non-invasive ventilation, etc.) have had success in prolonging ambulation and life expectancy of patients—increasing the average age of mortality from 15-19 to 30-35 [10,11]. However, with these increases in longevity, cardiac dysfunction has become the major cause of morbidity in DMD patients [12].

1.1.3 Clinical Symptoms of the Dystrophic Heart

Cardiovascular complications in DMD— typically dilated cardiomyopathy and cardiac arrhythmia—become detectable when the child reaches 10-12 years of age. A common misconception is that the dystrophic heart is clinically silent until the patient reaches puberty. However, pre-clinical signs of cardiomyopathy within patients—as young as 6 years of age—are abundant including sinus tachycardia and associated electrocardiograph abnormalities, right ventricle hypertrophy, and wall motion abnormalities in electrocardiograms. Around the age of 9-10, the first detectable signs of clinical cardiomyopathy emerge as myocardial fibrosis and left ventricle enlargement, which is then followed by ventricular dilation and dysfunction. From 10 years of age onwards, there is a rapid progression of both cardiac dysfunction severity and prevalence [6,13]. The number of cardiomyopathy symptomatic DMD patients increases from 26% at 10-14 years of age to 72% at 18 years of age. At end-stages, virtually all DMD patients will exhibit signs of cardiac abnormalities (i.e. conduction defects, arrhythmia, dilated or hypertrophic cardiomyopathy) until they eventually succumb to heart failure [13]. It should be noted that “typical” heart failure symptoms (e.g. orthopnea, dyspnoea, or exercise limitations) are often absent or hidden by skeletal muscle impairment in DMD, causing significant delays in evaluation and treatment [6,14].

1.1.4 Clinical Symptoms of the Dystrophic Brain

As DMD is a neuromuscular disorder, there are cognitive and neuropsychiatric implications associated with this disease. However, most literature prioritizes investigating the skeletal muscle degeneration associated with DMD, resulting in minimal knowledge on both cognitive and anatomical symptoms of the DMD brain. Additionally, the literature regarding the DMD brain is still heavily debated on and is often contradictory in nature. However, it is generally agreed upon that approximately 20-50% of DMD patients will exhibit cognitive and behavioural issues [15]. DMD boys are reported to have an increased likelihood of intellectual disabilities relative to both the general population and to their unaffected siblings—ruling out confounding socioeconomic factors (e.g. familial income, parent education level, etc.) [16]. Quantitatively, DMD patients typically have an average intelligence quotient (IQ) of approximately 85, which is one standard deviation below the average population. These reductions remain consistent when assessing Full Scale Intelligence Quotient tests (FSIQ), although these patients seem to demonstrate lower verbal IQ scores (VIQ) but not performance (PIQ). Both IQ and FSIQ scores in patients appear to be non-progressive as neither were observed to correlate with age nor disease severity [17,18].

While IQ and FSIQ are a good measure of general intelligence, it should be noted that DMD patients also suffer a specific pattern of cognitive and behavioural symptoms—albeit with considerable variability between individuals. Broadly, DMD patients can exhibit specific impairments in phonological awareness/processing, attention, visuo-spatial abilities, both verbal and visual working memory, and other executive functions (i.e. planning inhibition, set shifting, etc.) [17–19]. Cognitive impairments may manifest in school-aged DMD boys as limited vocabulary, poor language comprehension, inattention, weak working memory, and learning disabilities in reading, mathematics, and writing (i.e. dyslexia, dyscalculia, and dysgraphia) [20]. These deficits in cognitive function seem to persist during adulthood, as adult DMD patients (mean age of 30) seem to experience impaired attention, poor memory, and an inability to process auditory information [21]. DMD also shares brain-related comorbidities with the development of several other neurological and psychiatric disorders, such as an increased prevalence of

epilepsy (7.9%), autism spectrum disorders (15%), anxiety disorders, attention-deficit (hyperactivity) disorder (32%), and obsessive-compulsive disorders (4.8%). Interestingly, this is also found with transient neurological attacks [22]. For instance, in a retrospective review study of 59 males; patient records indicated that arterial ischemic stroke was more prevalent in DMD patients (occurring at an incidence of 1 per 100 patient years in comparison to current childhood ischemic stroke incidence of 1.6 per 100,000) [23,24]. At the same time, literature also indicates a high degree of inter-individual variability across cognitive symptoms between DMD patients. These symptoms cover a broad range of cognitive abilities—in which some are highly expressed, while others are nonexistent in particular individuals [17–19].

Similar aspects of heterogeneity are also prevalent within the anatomical architecture of DMD brains. For instance, some studies have indicated morphological abnormalities, while others suggest no gross structural differences between the dystrophic and healthy patient. In general, the dystrophin-deficient brains reportedly experience neuronal loss/reduced brain weight, gliosis, cerebral heterotopia, increased cortical thickness, and various alterations to brain microstructures (i.e. aberrant dendritic development and arborization, altered synaptic ultrastructure, etc.) [17,25–27]. However, these features are inconsistent and seem to vary between individuals. For instance, upon evaluating the post-mortem attributes of 13 DMD patient brains, the majority displayed no difference in brain weight nor gross anatomical structures. Despite no major anatomical differences, three patients within the study demonstrated histological dendritic abnormalities and arborization, while another patient demonstrated severe neuronal loss, astrogliosis, purkinje cell loss, and cerebral heterotopia [28]. While it is still uncertain if these morphological abnormalities are associated with impaired cognitive function, some neuroimaging studies have demonstrated decreased glucose metabolism within select regions of the dystrophic brain—which is typically indicative of cognitive impairment [17]. Interestingly, some studies have also indicated possible cerebral degeneration within DMD patients. For instance, using computer tomography (CT), Yoshioka et al. [29] observed that older DMD patients displayed more severe cerebral atrophy (i.e. enlarged internal and external cerebrospinal fluid space, abnormal cistern and sulci evaluation)

than the younger patients. Despite these investigations, no correlation was found between IQ, age, and DMD disease severity within these patients.

Historically cognitive symptoms appear to be non-progressive in DMD patients. However, recent studies have indicated that these cognitive deficits may progress, but its phenotype is only seen within older subsets of both DMD patients and animal models [21,30,31]. For instance, within a comparative executive function study using the Wisconsin Card Sorting Test (WCST), DMD patients (aged 30-37) had an average WCST score that was nearly 50% lower than their younger DMD counterparts (age 18-25) [30]. These results were consistent within aged *mdx* mice (age 18 months), as they displayed decreased hippocampal spatial learning, impaired memory, and heightened anxiety-related behaviour compared to their younger counterparts (age 4 months) [31]. This indicates that with increasing age, DMD patients may experience delayed-onset neurodegeneration, possibly further hindering the quality of the later stages of their lives.

Thus, due to the improved management of skeletal and respiratory dysfunctions, more patients are now surviving long enough for the emergence of heart failure and cognitive impairment associated with the later stages of the disease. With this increased longevity in DMD patients, the clinical relevance of downstream cardiac and neurodegeneration become abundant, increasing the need for a better understanding of both cardiac and neurological involvement. As such, this thesis will primarily focus on the dystrophic heart and brain.

1.2 Pathophysiology

1.2.1 Overview of Dystrophin

The *DMD* gene, notably the largest gene in the human body, contains nearly 2.5 million DNA base pairs and 80 exons. Being tightly regulated by sets of internal promoters, it produces a diverse plethora of protein isoforms (called dystrophin protein variants) with unique functions specific to various tissues of the body (e.g. retina, skeletal and cardiac muscle, brain, schwann cells, etc). Examples of these dystrophin protein variants include full length dystrophin Dp427 (mainly expressed in skeletal and cardiac muscle), and

Dp140 and Dp71 (mainly expressed in the brain) [12,25,32]. Duchenne muscular dystrophy arises due to a mutation in any region within the *DMD* gene, with the most common being a frameshift mutation due to a deletion of one or more exons. The lack of functional dystrophin, within several regions of the body, can lead to various symptoms as this disorder simultaneously affects multiple organs—further building on DMD's reputation as a systemic disease [12,33].

1.2.2 Dystrophic Cardiac Pathology

Dp427 is the resident dystrophin isoform within the skeletal and cardiac muscle, specifically located on the inner side of the sarcolemma within myocytes. It is hypothesized that dystrophin forms the dystrophin-associated protein complex (DAPC) along with other transmembrane proteins (i.e. dystroglycans, sarcoglycans, etc.), and serves as a link between the cytoskeletal actin filaments, contractile units of myofibers, and the extracellular matrix' laminin protein (Figure 1.1). As such, dystrophin mechanically stabilizes the plasma membrane during contraction by transferring the forces generated by the sarcolemma to the extracellular matrix. In addition, dystrophin (and the DAPC) is also integral in enabling signal transduction between the intra- and extracellular environment. A notable example is neuronal nitric oxide synthase (nNOS), which is localized to the sarcolemma by dystrophin. This facilitates the nitric oxide (NO) synthesis signaling pathway and subsequently signals blood vessels dilation, allowing the passage of oxygen and nutrients to muscle cells [34–36].

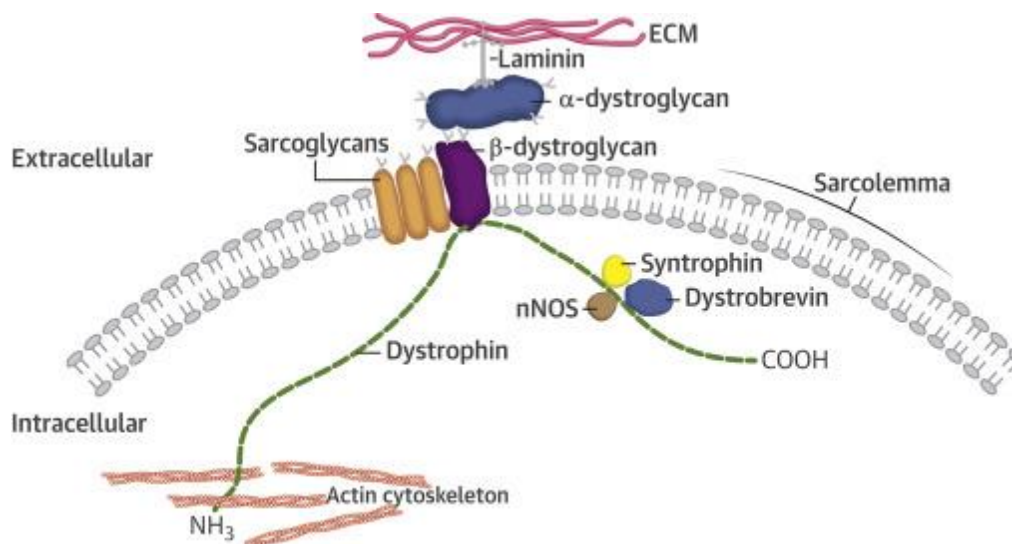


Figure 1.1 Dystrophin serves as an integral component of the Dystrophin-associated protein complex (DAPC) and links the actin cytoskeleton to extracellular matrix (ECM). Schematic displays the binding of the actin cytoskeleton-bound dystrophin to DAPC transmembrane proteins (i.e. sarcoglycan, dystroglycans), which anchors laminin-bound ECM. This complex serves to stabilize the sarcolemma during muscle contraction. Dystrophin may also interact with additional proteins (i.e. nNOS) at the sarcolemma, allowing for signal transduction [35].

Within dystrophinopathies, there are many theories for the degeneration of cardiac muscle. Among them is the “two-hit” hypothesis model, which speculates that the dystrophic phenotype is not caused by one exclusive mechanism, but rather the cumulative effects of multiple stressors. In this model, the first “hit” is the destabilization of the DAPC. During DMD, the absence of dystrophin (and associated DAPC) causes the muscle cells to be vulnerable to mechanical stress, increasing the susceptibility of the cells to damage during cardiac muscle contractions. As a result, contractile forces cause the shearing and tearing of the sarcolemma membrane [4,34,37]. Immune cells (i.e. neutrophils, mast cells, and macrophages) are recruited to the sites of mechanical damage to help with phagocytosis of cell debris and to release inflammatory cytokines that can instigate myonecrosis [5,38]. Additionally, the myocyte’s tearing can increase membrane permeability, causing an abnormal influx of calcium ions from the extracellular space into the cell. Furthermore, this dysfunctional calcium influx may be a result of impairments to the L-type calcium channels and mechanical stretch-activated receptors—which regulates the depolarization and contraction of the cardiomyocyte via calcium ions.

This intracellular calcium causes further problems as it can activate proteases (e.g. calpain), which are thought to degrade a wide variety of contractile proteins and induce myocyte necrosis [36,38,39].

The second “hit” is often described as damage that is environmentally or indirectly induced [12]. For instance, the excess calcium levels within myocytes were also found to trigger the release of reactive oxygen species (ROS). In cardiac muscle, ROS promotes inflammatory cell recruitment by activating inflammatory signaling pathways (i.e. NF- κ B) and releasing pro-inflammatory cytokines [38,41–43]. These immune cells (e.g. M1-like and M2-like macrophages, neutrophils, T-cells, etc.) are recruited and typically found at the site of cardiac injury [44]. In particular, pro-inflammatory macrophages are thought to attack cardiac myofibers and exacerbate the myonecrosis process upon chronic activation, further damaging the sarcolemma [5,38,45]. Additionally, ROS can trap these macrophages at the site of inflammation by upregulating cytokine macrophage migration inhibitory factor—prolonging the damage [46]. During this myonecrosis process, these inflammatory macrophages can also release pro-inflammatory cytokines, which may trigger fibroblasts to produce collagen in the extracellular matrix. Increased collagen deposition is notably dangerous, as it leads to fibrosis—particularly in regions of high contractility and movement (e.g. left ventricle). As a result, elastic cardiac muscle is replaced with segments of rigid fibrotic tissue, which can cause pre-clinical symptoms of cardiomyopathy such as conduction defects or decreased systolic ejection [38,39,44].

Ischemic injury, caused by the mislocalization of neuronal nitric oxide synthase (nNOS), can also contribute to acute myocyte death. nNOS is normally bound to the sarcolemma by the DAPC. Thus, with dystrophin’s absence, nNOS is unanchored and will localize to the cytosol. This process causes vasoconstriction of the blood vessel—leading to inadequate blood flow, poor oxygen regulation, and ultimately muscle ischemia. The rapid accumulation of inflammatory cells to the site of ischemic injury may also lead to the induction of myonecrosis [47–49].

In summary, current literature dictates that the DMD cardiac phenotype is the product of several complex and multi-faceted cascades arising from the dystrophin protein

dysfunction. While mechanical injury and membrane defects are thought to be the initial causes of DMD, secondary mechanisms encompassing chronic inflammation, fibrosis, and ischemia also seem to contribute to this defective pathophysiology. Thus, a better understanding and tracking of these secondary mechanisms—specifically inflammation—may lead to a better understanding of cardiac outcomes.

1.2.3 Dystrophic Neural Pathology

Unlike the full-length dystrophin (Dp427) found in cardiac and skeletal muscle, dystrophin within the brain are expressed as several protein isoforms of varying lengths. Different isoforms (e.g. Dp427, Dp140, and Dp71) are localized to specific brain regions/cells and participate in various cellular functions. For instance, Dp427 typically localizes to the neurons in the cerebellum, cortex, and hippocampus, while Dp71 typically localizes to astrocytes and glial cells [25,32,50]. While the etiology behind DMD patients' cognitive symptoms remain unknown, it is suspected to be caused by a mutation to certain regions of the *DMD* gene leading to the loss of one or more dystrophin protein isoforms [25]. For instance, in a large genetic study containing 65 DMD patients, the risk of cognitive deficit—portrayed by FSIQ scores—is highly correlated to gene location and the resultant types of isoforms lost. Here, patients who had lost the shorter isoforms (i.e. Dp71) yielded the lowest FSIQ compared to those who lost only the longer isoforms (i.e. full-length Dp427) [51]. As such, the heterogeneity of DMD cognitive dysfunction is thought to be caused by the cumulative loss of different dystrophin isoforms.

Unfortunately, the exact function of each dystrophin protein variant within the brain is still vastly uncharacterized. Within murine models, Dp427 has been found to colocalize with a subset of γ -aminobutyric acid (GABA_A)—a neurotransmitter important for the regulation of learning and memory— receptors clusters within the synaptic regions of the cerebellum, cerebral cortex, and hippocampus [50,52,53]. Alike to muscle cells, Dp427 is suspected to be integral to the formation of DAPC-like structures within the brain, which may aid in the stabilization/anchoring of GABA_A receptors to the neuronal post-synaptic membranes [54]. In support of this, *mdx* mice were observed to have a notable reduction

in the number of GABA_A receptor clusters in the cerebellum [53]. As such, Dp427 may play a role in maintaining GABAergic synaptic function. The loss of Dp427 may alter signal transduction/synaptic plasticity, leading to learning/memory deficits seen in DMD patients [54,55].

Despite being the most abundant dystrophin protein variant in the adult brain, Dp71 typically localizes to perivascular end-feet of astrocytes and clusters of water channel protein aquaporin-4 (AQP4) receptors [32,56]. Both of these structures are important in maintaining the blood-brain barrier (BBB). Astrocytes' end-feet processes interact with endothelial cells and pericytes form tight junctions to restrict the entry of non-specific molecules from circulation into the brain. On the other hand, AQP4 channels control water influx into the brain. Thus, it is suspected that Dp71 may contribute to the modulation of BBB permeability [32,57,58]. While the exact role of dystrophin protein within the BBB has yet to be confirmed, several investigators have demonstrated its importance in maintaining BBB function/vascular permeability through several DMD murine studies. For instance, Nico et al. [58] observed that the BBB of *mdx* adult mice—a murine model of DMD—suffered severe damage and subsequently disrupted. Most notably, the authors histologically observed increased vascular permeability, less endothelial tight junction protein expression, decreased AQP4 protein, and the emergence of swollen and degenerating perivascular end-feet, marked by a discontinuous envelopment of endothelial vessels. Similar incidences of disrupted BBB integrity and cerebral diffusivity were confirmed to occur *in-vivo* in *mdx* mice [59]. To the best of my knowledge, the correlation between BBB disruption and cognitive impairment within DMD has yet to be studied. However, it is common for BBB breakdown to initiate cognitive impairment within several other neurodegenerative diseases (e.g. Alzheimer's dementia, Parkinson's disease, and multiple sclerosis) [60]. Interestingly, an altered BBB integrity coupled with increased neuroinflammatory infiltration is thought to contribute to the increased risk of Autism spectrum disorder and epilepsy—both common comorbidities in DMD patients [61,62]. As such, it is possible that the altered BBB permeability seen in DMD mice is also associated with neuroinflammation, which in turn can contribute to the emergence of DMD cognitive impairment and neurodegenerative symptoms.

Although chronic inflammation is a key component of DMD muscle pathophysiology, only recently has there been increasing consideration of neuroinflammation's contribution to cognitive impairment within this disease [54,63]. In a recent study, *mdx* mice who exhibited DMD-like cognitive symptoms (i.e. impaired memory, depression- and anxiety-like behaviour) also had elevations of pro-inflammatory cytokines (i.e. IL-1 β and TNF α) and increased MPO activity (an analog for inflammation and leukocyte infiltration) in their brains [64]. In support of this, two speculative reviews propose that these pro-inflammatory cytokines are likely to disrupt hippocampal function in dystrophinopathies, which facilitates learning/memory processing. For example, the upregulation of IL-1 β is speculated to modify GABAergic synaptic transmission by altering the expression of inhibitory hippocampal GABA_A receptors—features that are typically observed in *mdx* mice. Although the mechanisms underlying these inflammation-induced memory deficits are not well-understood, it is proposed that such alterations may result in the increased potentiation of GABAergic inhibitory currents, which is associated with memory deficits [54,63]. Thus, although the current literature outlining inflammation's role in dystrophic neuropathy are few and speculative in nature, these findings highlight the potential role of immune molecules in modulating neurologic function within the dystrophic brain.

1.3 Inflammation Contributes to DMD Cardiac and Neurologic Outcomes

While dystrophin-absent mechanical injury and membrane defects are thought to be proximate causes of DMD, secondary mechanisms (such as chronic inflammation, fibrosis, and ischemia) also contribute to the defective pathophysiology [5]. As previously discussed in 1.2.1, chronic inflammation is an imperative component in DMD cardiac muscle pathogenesis—as sarcolemma damage causes the recruitment of activated glial cells and the secretion of pro-inflammatory cytokines. Due to the multitude of signaling pathways and its participants, the mechanism to how inflammation affects DMD muscle pathophysiology is highly complex. While the mechanism underlying how each individual participant (e.g. neutrophils, M1-like and M2-like macrophages,

inflammatory cytokines, etc.) affects dystrophic muscle remains unclear, they all cumulatively contribute to the development of cardiomyopathy and possibly the eventual emergence of heart failure [5]. In particular, macrophages are thought to have a central role in exacerbating dystrophic muscle damage—since an abundance of macrophages and neutrophils were shown to localize to regions of cardiac necrosis/lesions in immunohistochemical staining of dystrophic mice hearts [45]. In addition, *mdx* models with a predisposition for inflammation demonstrated extensive M1-like macrophage infiltration and more severe cardiorespiratory dysfunction (i.e. decreased fractional shortening and ejection fraction) compared to normal *mdx* models [38]. After removing the macrophages from the muscle prior to the onset of myocyte necrosis (3-4 weeks), *mdx* mice will later have a 70-80% decrease in number of injured muscle fibers (~3 months of age) [65]. These findings further demonstrate the importance of inflammation in dystrophic cardiac outcome, emphasizing the need to better assess its presence in DMD models as its attenuation may aid in slowing down cardiac dysfunction.

Similarly, neuroinflammation—depicted as heightened pro-inflammatory cytokines—in the dystrophic brain is increasingly considered to be a contributor of cognitive impairment associated with this disorder [54,63]. While much about this hypothesis remain unclear, activated microglia—which commonly acts as the source and target of these inflammatory cytokines—are implicit in the development of several other neuroinflammatory and degenerative diseases, such as: Alzheimer’s dementia (AD), Parkinson’s disease, and frontotemporal dementia [66]. Interestingly, activated microglia have also emerged as a prime component of late-onset AD, in which similar to DMD, the clinical symptoms of cognitive degeneration do not emerge until the later stages of life [67]. To the best of my knowledge, no study thus far has demonstrated the presence of activated microglia within the dystrophic brain. However, with this information and a better understanding of neuroinflammation in DMD, there is the potential to develop anti-inflammatory neuroprotective therapies that may improve patient’s cognitive function at the later stages of this disease.

Due to the potential consequences of unchecked inflammation on the heart and brain, there is a need to better understand the role of inflammation in multi-organ

degeneration—as it may lead to the subsequent development of effective therapeutic strategies that targets multiple bodily systems, especially brain and heart resilience in DMD patients. However, a valid assessment tool must be developed in order to track inflammatory status within several organs—especially in the heart and brain of DMD patients.

1.4 Assessments of Inflammation

As previously discussed in section 1.3, inflammation holds a great deal of importance as not only a localized response to tissue/organ injury, but also as a potential contributor to downstream cardiac and neurological outcomes. As such, the assessment of inflammatory response within DMD could aid in tracking disease progression and in developing effective therapeutic strategies targeted to before the onset of severe cardiac or neurological damage. Currently inflammation is not routinely monitored during clinical DMD progression assessments. However, in other diseases, inflammatory load can be assessed *ex-vivo* using in-fluid circulating inflammatory markers (i.e. C-reactive protein, IL-6, etc.) and histopathological trafficking of immune cells, or *in-vivo* via non-invasive molecular imaging [68]. Similar applications can foreseeably be done in DMD.

1.4.1 *Ex-vivo* Assessments

It is well-established in literature that inflammation can be assessed through several different methods, ranging from: the novel inflammation-on-a-chip devices (an *ex-vivo* contraption that uses microfluidic tools to visualize cellular events in a controlled tissue microenvironment) to the more traditional and clinically-used biomarkers such as: inflammatory cytokines (e.g. IL-6, TNF- α , IL-1 β) and acute phase proteins (e.g. C-reactive protein) [68,69]. Cytokines are secreted by immune cells (i.e. activated macrophages and monocytes) at the site of inflammatory injury. However, they are also found within circulation as they are crucial mediators of both local and systemic reactions, allowing them to be contributors to the aetiology of chronic diseases [70]. Similarly, C-reactive protein (CRP) exhibit elevated expression during inflammatory conditions in cardiovascular and cerebrovascular diseases [71,72]. These molecules can

be significantly upregulated in response to tissue-induced inflammatory activity within 24 to 48 hours after initial insult [73]. These circulating inflammatory markers can be measured *ex-vivo* by analyzing plasma/serum from blood or from other invasive locations (e.g. saliva, urine, and cerebrospinal fluid). The use of in-fluid biomarkers is advantageous because they are simple, fast to conduct, and are able to evaluate an inflammatory or infectious state [74]. However, inter-individual genetic variations can specifically increase plasma CRP levels regardless of inflammatory status, limiting its sensitivity and specificity [73,74]. In addition, it does not identify the source nor target of the inflammatory response, leaving little information on which organ(s) are damaged. As such, despite in-fluid biomarkers' ability to assess inflammatory status, it is limited in its identification of the inflammatory location.

On the other hand, tissue-specific inflammatory information in the heart and brain can be acquired *ex-vivo* with endomyocardial and brain biopsies. The removed segments of neural and cardiac tissue are often histologically stained and microscopically examined, allowing us to visualize and assess the extent and exact location of the inflammatory infiltrate with a high degree of specificity [75,76]. However due to its invasive nature, the amount of tissue obtained is minimal and thus, may not be representative of the whole organ's pathological status [77]. In addition, the localized nature of invasive tissue biopsies is a concern within DMD assessment since DMD is a whole-body systemic disease. This limitation can be extended to most *ex-vivo* vectors. As such, tissue biopsies may be insufficient in observing inflammatory load within multiple organs simultaneously without extensive surgical procedure, and the information obtained may not even be indicative of that organ's pathological state.

1.4.2 *In-vivo* Assessments

In-vivo imaging technology is understandably better suited than *ex-vivo* technology in observing the overall inflammatory effects on a living subject in real time. In regard to inflammatory imaging, there are a few alternatives that can be considered. For instance, magnetic resonance imaging (MRI) has been used to evaluate the pathogenesis of several inflammatory disorders and to study cardiac involvement in DMD patients [78,79]. This

imaging modality uses an external magnetic field to first align the typically randomly-oriented hydrogen within water molecules in the subject. Various external radiofrequency (RF) energies—also known as RF pulse sequences—are applied, resulting in the excitation of the aligned proton atoms. Upon their relaxation from this excited state, the proton will emit signals that are detected and recorded both temporally and spatially by the scanner. These signals are then transformed, resulting in a high-quality anatomically and structurally accurate image. Depending on the RF pulse sequence applied and the detected relaxation time of the excited proton (known as T1- and T2- relaxation times), different functional information can be inferred. Conventionally T2 relaxation times are increased in tissue lesions or regions of edema (often associated with elevated inflammation)—resulting in these regions appearing brighter than surrounding normal tissue in MR images [79]. As a result, T2-relaxation time mapping is used to determine the pathologic state of the affected tissue, while allowing us to identify the organ of damage/region of inflammatory infiltration within the affected subject. In contrast to *ex-vivo* assessment tools, MRI can not only identify abnormal pathophysiology in tissue-specific regions, but can also image the entire body—allowing us to acquire information regarding multiple organs simultaneously in one scan. While T2-weighted imaging has been successful in differentiating between the muscle of DMD and healthy patients, its specificity as a marker of inflammation is limited due to the confounding influence of edema or fat infiltration [80,81]. In addition, inflammatory foci are virtually undetectable in the earlier stages of disease progression if no blatant anatomical changes are present. In summary, T2-weighted MRI may be a useful tool for the body-wide assessment of DMD, but it is limited by its specificity and sensitivity in detecting inflammation.

Another imaging modality is positron emission tomography (PET). PET is a non-invasive imaging technique that relies on the *in-vivo* detection of a radioactive tracer—also known as a radiotracer—as it binds specifically to a region/receptor of interest. A radiotracer, by definition, is the radioactive element-labelled (e.g. ^{18}F , ^{11}C , or ^{15}O) ligand or substrate that are highly specific for that targeted enzyme or receptor within the body. It is due to this ligand-binding specificity that gives PET its identity as a molecular imaging modality, as it can visualize and measure these biological processes at molecular and cellular levels [82]. As such, PET offers higher sensitivity as it can detect imaging agents

at a 10^{-11} - 10^{-12} molar level in contrast to MRI (at approximately 10^{-3} - 10^{-5} molar) and CT (at approximately 10^{-2} - 10^{-3} molar) [83]. To conduct PET imaging, a tracer is administered (usually by injection or inhalation). Depending on the positron-emitting radioisotope bound to the tracer, a specific percentage of the nuclei will decay by emitting positrons. These positrons generally travel a certain distance before colliding or annihilating with an electron, resulting in the production of two 511keV photons that are expelled at a 180° angle. Using opposing detectors within the scanner, the detection of these expelled photons in coincidence allows for the localisation of the source of this emission (i.e. the tracer) and tracer activity concentration within the subject. Thus, alike to MRI, this imaging modality allows us to identify regions of affected pathophysiology simultaneously in multiple organs in real time from a single scan. However, unlike MRI, PET can identify the presence of inflammation at a much higher specificity depending on the radiotracer of choice. To the best of my knowledge, there has yet to be a study conducted with the goal of imaging inflammation in DMD using PET. However, this imaging modality may be useful in assessing inflammatory status *in-vivo* as it has already successfully demonstrated its utility in several other inflammatory disorders (e.g. cardiac sarcoidosis, vasculitis, and rheumatoid arthritis) [84].

1.5 Inflammatory PET Radiotracers

1.5.1 Glucose-metabolism Analogue Tracer – FDG

The most extensively used radiotracer within both the research and clinical environment is 2-deoxy-2- ^{18}F -fluoro-D-glucose (^{18}F -FDG), a glucose analogue that allows for the quantification of glucose metabolism within metabolically active cells/tissues. While not a direct marker of inflammation, it has shown significant value for successful imaging of cardiac and neural inflammatory diseases, such as atherosclerosis, vasculitis, Alzheimer's dementia, and multiple sclerosis [85,86]. This can be attributed to the fact that immune cells—in particular macrophages/microglia and neutrophils—have an increased demand for glucose than peripheral non-inflammatory cells. As such, sites of significant [^{18}F]FDG uptake can be used to identify regions of activated macrophage accumulation [83,87]. However, the imaging of inflammation with [^{18}F]FDG PET has the tendency to

yield false-positive results (e.g. accumulating in metabolically active benign tumors or brown adipose tissue) [88,89]. In addition, the heart and brain are naturally very metabolically-active organs. As a result, there is a higher level of tracer accumulation within those areas, making it difficult to detect inflammatory infiltrates in those areas without it being obscured by background activity [83,88]. Thus, there has been increasing reliance on more specific inflammatory radiotracers that target macrophage or microglia directly.

1.5.2 Translocator Protein (TSPO) Tracer – FEPPA

One candidate that has been increasingly used to image inflammation are radiotracers that bind to translocator protein (TSPO). Also known as peripheral benzodiazepine receptor (PBR), TSPO is a 18kDa transmembrane protein located on the outer membrane of mitochondria, and is constitutively expressed at low-to-moderate levels in several organs (e.g. kidneys, adrenal glands, lungs, and the healthy myocardium and brain parenchyma) [90]. Specifically, within the healthy brain, TSPO is also expressed at minimal amounts on resting microglial cells [91]. However, during cases of neurological disease/injury and inflammation, TSPO is considerably upregulated specifically on activated microglia and reactive astrocytes [92,93]. In fact, several studies have indicated a colocalization of TSPO overexpression and activated microglia in both acute injury and chronic degenerative disorders—including multiple sclerosis, Parkinson's and Alzheimer's dementia [92,94]. For instance, audioradiograms and confocal microscopy demonstrated that sites of TSPO-tracer binding overlapped with regions rich in CD68-stained activated macrophages and microglia nodules in brain sections of macaques suffering from simian immunodeficiency virus encephalitis [95]. As such, TSPO-PET is highly used in research for the detection of regions particularly abundant in microglia activation, which are typically regions associated with neuronal damage.

Recently, TSPO-PET radiotracers have been increasingly used outside of the neural environment to image inflammation in peripheral organ diseases. Despite its ubiquitous expression in several tissues, several studies have demonstrated significantly higher levels of TSPO expression in peripheral organs during disease-induced inflammation than

that of healthy controls [91,96]. For instance, the myocardium of experimental autoimmune myocarditis models demonstrated an approximate 3.7-fold higher level of TSPO expression than that of healthy controls. These areas of increased TSPO expression were also colocalized immunohistochemically with regions highly concentrated with CD68+ macrophages [97]. Likewise, autoradiography and immunohistostaining of a murine CD68+ carotid, and fibrotic human carotid tissue samples indicated TSPO-tracer localization within inflamed and damaged areas [98,99]. Furthermore, [¹¹C]PK11195—another TSPO radiotracer—has been successfully used to image both cardiac and neuroinflammation within a patient post-myocardial infarction, demonstrating TSPO-PET's feasibility as a multi-organ inflammation-investigative tool [94]. Thus, the PET imaging of TSPO in both activated macrophages and microglial cells, may be sensitive enough for the *in-vivo* detection and quantification of inflammation body-wide within DMD.

Currently there are several TSPO-associated radiotracers used in literature that have successfully imaged both cardiac and neuroinflammation across several diseases [91,96]. Examples of these include: the historic [¹¹C]-(*R*)-(2-chlorophenyl)-*N*-methyl-*N*-(1-methylpropyl)-3-isoquinoline-carboxamide ([¹¹C]PK11195), and the second generation tracer [¹⁸F]-*N*-(2-(2-fluoroethoxy)benzyl)-*N*-(4-phenoxy pyridin-3-yl)acetamide ([¹⁸F]FEPPA) [100,101]. [¹¹C]PK11195 is the most widely studied and has vastly contributed to delineating the role of inflammation in several acute and degenerative disorders [102,103]. However, there is an increasing reliance on second generation TSPO radiotracers (e.g. [¹⁸F]FEPPA) as they resolve some of the challenges associated with [¹¹C]PK11195—such as short half-life of ¹¹C, better brain penetration, and increased specificity [104,105]. Having been radiolabeled with ¹⁸F, these TSPO radiotracers have a longer half-life of 109.8 minutes, allowing for more extensive research with relatively less temporal restriction. In addition, [¹⁸F]FEPPA has comparatively better binding potential, specificity, and penetrative ability of the BBB than [¹¹C]PK11195—thereby being a better *in vivo* assessment tool for inflammation in both the dystrophic heart and brain [106].

1.6 Pre-clinical Murine Models of DMD

There is an abundance of animal models for DMD, ranging from small non-mammalian *Drosophila melanogaster* to larger newly developed pig models. However, rodent models remain one of the most widely used vectors due to their genotypic and pathological resemblance to DMD-diagnosed humans. Amongst the many strains is the *mdx* mouse, which has no functional dystrophin protein due to a point mutation in the X-chromosome of the *DMD* gene so that like its human counterpart, will possess no functional dystrophin protein [107]. As a result, this murine model can demonstrate histopathological characteristics of tissue degeneration and inflammatory infiltrate within skeletal muscle [108]. In addition, *mdx* mice also exhibited signs of cognitive dysfunction in the form of impaired visuospatial memory, impaired avoidance memory, anxiety, and depressive behaviours within 8 weeks of age [64,109,110]. In addition, they are known to exhibit a reduced capacity to learn and store spatial memories [109,111]. However, this strain's efficacy is greatly decreased as they exhibit none or mild non-progressive cardiomyopathy even after 10 months of age—despite showing a degree of inflammation, cellular necrosis, and fibrosis within their myocardium [112]. This can be attributed to the compensatory effects of dystrophin protein homolog, utrophin. Unlike their human counterparts, utrophin in *mdx* mice can substituted structurally for dystrophin within muscle—restoring DAPC and subsequently leading to an improved muscle pathology [113].

On the other hand, the *mdx:utrn(+/-)* mouse is able to exhibit a slightly more severe phenotype as it only possesses one functional copy of the utrophin protein. For instance, both skeletal and cardiac muscle of *mdx:utrn(+/-)* models exhibit more severe collagen deposition and fibrosis than that of *mdx* mice [114]. As such, it is often referred to in literature as a more accurate model of DMD phenotypically. To the best of my knowledge, the cognitive impact within the *mdx:utrn(+/-)* model has yet to be characterized. However, as these models depict a more severe phenotype, they are predicted to show greater cognitive impairment than within the *mdx* model.

1.7 Research Outline

Within this thesis, *mdx:utrn*(+/-) mice were utilized. Specifically, 8-10 week old murine models were selected, as evidence of cognitive impairment and early signs of cardiac fibrosis (but not cardiomyopathy symptoms) have been reported at this age [64,115]. This age group may provide information about inflammation prior to severe tissue damage. After an injection with [¹⁸F]FEPPA, PET images were taken of the whole body to better assess inflammatory load collectively on a multi-organ level. In order to validate the [¹⁸F]FEPPA PET data and quantify TSPO-tracer *ex-vivo*, autoradiography and biodistribution were conducted on not only the heart and brain but also several peripheral organs. Autoradiography was conducted on the thoracic and abdominal aorta, heart, brain, gastrocnemius, soleus, extensor digitorum longus, tibialis anterior, and liver. In addition to these tissues, biodistribution was also conducted on the large intestine, small intestine, diaphragm, tibia/fibula, tail, pancreas, lungs, and spleen. These data provide a better understanding of inflammation on a systemic level. Immunohistochemical staining with anti-TSPO antibody was also examined to further validate if the TSPO-tracer is localizing to the cardiac and neural tissue.

1.7.1 Study Objectives

1. To develop a non-invasive imaging protocol to assess *in vivo* inflammatory involvement in DMD simultaneously in several organs using [¹⁸F]FEPPA PET
2. To investigate the role of inflammation in the heart and brain of DMD murine models

1.7.2 Study Hypothesis

We hypothesized that subjects with DMD demonstrated heightened levels of inflammation in dystrophic cardiac and neural tissues.

1.8 References

- [1] Bushby K, Finkel R, Birnkrant DJ, Case LE, Clemens PR, Cripe L, et al. Diagnosis and management of Duchenne muscular dystrophy, part 1: diagnosis, and pharmacological and psychosocial management. *Lancet Neurol* 2010;9:77–93. [https://doi.org/10.1016/S1474-4422\(09\)70271-6](https://doi.org/10.1016/S1474-4422(09)70271-6).
- [2] Grimm T, Kress W, Meng G, Muller CR. Risk assessment and genetic counseling in families with Duchenne muscular dystrophy. *Acta Myol* 2012;31:179–83.
- [3] Lee T, Takeshima Y, Kusunoki N, Awano H, Yagi M, Matsuo M, et al. Differences in carrier frequency between mothers of Duchenne and Becker muscular dystrophy patients. *J Hum Genet* 2014;59:46–50. <https://doi.org/10.1038/jhg.2013.119>.
- [4] Davies KE, Nowak KJ. Molecular mechanisms of muscular dystrophies: old and new players. *Nat Rev Mol Cell Biol* 2006;7:762–73. <https://doi.org/10.1038/nrm2024>.
- [5] Rosenberg AS, Puig M, Nagaraju K, Hoffman EP, Villalta SA, Rao VA, et al. Immune-mediated pathology in Duchenne muscular dystrophy. *Sci Transl Med* 2015;7:299rv4. <https://doi.org/10.1126/scitranslmed.aaa7322>.
- [6] D'Amario D, Amodeo A, Adorisio R, Tiziano FD, Leone AM, Perri G, et al. A current approach to heart failure in Duchenne muscular dystrophy. *Heart* 2017;103:1770–9. <https://doi.org/10.1136/heartjnl-2017-311269>.
- [7] Eagle M, Baudouin SV, Chandler C, Giddings DR, Bullock R, Bushby K. Survival in Duchenne muscular dystrophy: improvements in life expectancy since 1967 and the impact of home nocturnal ventilation. *Neuromuscul Disord* 2002;12:926–9. [https://doi.org/10.1016/S0960-8966\(02\)00140-2](https://doi.org/10.1016/S0960-8966(02)00140-2).
- [8] Verma S, Anziska Y, Cracco J. Review of Duchenne Muscular Dystrophy (DMD) for the Pediatricians in the Community. *Clin Pediatr (Phila)* 2010;49:1011–7. <https://doi.org/10.1177/0009922810378738>.
- [9] Guiraud S, Aartsma-Rus A, Vieira NM, Davies KE, van Ommen G-JB, Kunkel LM. The Pathogenesis and Therapy of Muscular Dystrophies. *Annu Rev Genomics Hum Genet* 2015;16:281–308. <https://doi.org/10.1146/annurev-genom-090314-025003>.
- [10] Bushby K, Finkel R, Birnkrant DJ, Case LE, Clemens PR, Cripe L, et al. Diagnosis and management of Duchenne muscular dystrophy, part 2: implementation of multidisciplinary care. *Lancet Neurol* 2010;9:177–89. [https://doi.org/10.1016/S1474-4422\(09\)70272-8](https://doi.org/10.1016/S1474-4422(09)70272-8).

- [11] Babbs A, Chatzopoulou M, Edwards B, Squire SE, Wilkinson IVL, Wynne GM, et al. From diagnosis to therapy in Duchenne muscular dystrophy. *Biochem Soc Trans* 2020;48:813–21. <https://doi.org/10.1042/BST20190282>.
- [12] McNally EM. New Approaches in the Therapy of Cardiomyopathy in Muscular Dystrophy. *Annu Rev Med* 2007;58:75–88. <https://doi.org/10.1146/annurev.med.58.011706.144703>.
- [13] Nigro G, Comi LI, Politano L, Bain RJ. The incidence and evolution of cardiomyopathy in Duchenne muscular dystrophy. *Int J Cardiol* 1990;26:271–7. [https://doi.org/10.1016/0167-5273\(90\)90082-g](https://doi.org/10.1016/0167-5273(90)90082-g).
- [14] Birnkrant DJ, Bushby K, Bann CM, Alman BA, Apkon SD, Blackwell A, et al. Diagnosis and management of Duchenne muscular dystrophy, part 2: respiratory, cardiac, bone health, and orthopaedic management. *Lancet Neurol* 2018;17:347–61. [https://doi.org/10.1016/S1474-4422\(18\)30025-5](https://doi.org/10.1016/S1474-4422(18)30025-5).
- [15] Cotton S, Voudouris NJ, Greenwood KM. Intelligence and Duchenne muscular dystrophy: Full-Scale, Verbal, and Performance intelligence quotients. *Dev Med Child Neurol* 2007;43:497–501. <https://doi.org/10.1111/j.1469-8749.2001.tb00750.x>.
- [16] Hinton VJ, Vivo DCD, Nereo NE, Goldstein E, Stern Y. Selective deficits in verbal working memory associated with a known genetic etiology: The neuropsychological profile of Duchenne muscular dystrophy. *J Int Neuropsychol Soc* 2001;7:45–54. <https://doi.org/10.1017/S1355617701711058>.
- [17] Snow WM, Anderson JE, Jakobson LS. Neuropsychological and neurobehavioral functioning in Duchenne muscular dystrophy: a review. *Neurosci Biobehav Rev* 2013;37:743–52. <https://doi.org/10.1016/j.neubiorev.2013.03.016>.
- [18] Bresolin N, Castelli E, Comi GP, Felisari G, Bardoni A, Perani D, et al. Cognitive impairment in Duchenne muscular dystrophy. *Neuromuscul Disord NMD* 1994;4:359–69. [https://doi.org/10.1016/0960-8966\(94\)90072-8](https://doi.org/10.1016/0960-8966(94)90072-8).
- [19] Ueda Y. Cognitive Function and Quality of Life of Muscular Dystrophy. *Muscular Dystrophies* 2019. <https://doi.org/10.5772/intechopen.86222>.
- [20] Learning & Behavior. Parent Proj Muscular Dystrophy n.d. <https://www.parentprojectmd.org/care/care-guidelines/by-area/learning-and-behavior/> (accessed August 20, 2020).
- [21] Ueda Y, Suwazono S, Maedo S, Higuchi I. Profile of cognitive function in adults with duchenne muscular dystrophy. *Brain Dev* 2017;39:225–30. <https://doi.org/10.1016/j.braindev.2016.10.005>.
- [22] Hendriksen JGM, Vles JSH. Neuropsychiatric disorders in males with duchenne muscular dystrophy: frequency rate of attention-deficit hyperactivity disorder

- (ADHD), autism spectrum disorder, and obsessive-compulsive disorder. *J Child Neurol* 2008;23:477–81. <https://doi.org/10.1177/0883073807309775>.
- [23] Winterholler Martin, Holländer Christian, Kerling Frank, Weber Irina, Dittrich Sven, Türk Matthias, et al. Stroke in Duchenne Muscular Dystrophy. *Stroke* 2016;47:2123–6. <https://doi.org/10.1161/STROKEAHA.116.013678>.
- [24] Mallick AA, Ganesan V, Kirkham FJ, Fallon P, Hedderly T, McShane T, et al. Childhood arterial ischaemic stroke incidence, presenting features, and risk factors: a prospective population-based study. *Lancet Neurol* 2014;13:35–43. [https://doi.org/10.1016/S1474-4422\(13\)70290-4](https://doi.org/10.1016/S1474-4422(13)70290-4).
- [25] Doorenweerd N. Combining genetics, neuropsychology and neuroimaging to improve understanding of brain involvement in Duchenne muscular dystrophy - a narrative review. *Neuromuscul Disord* 2020;30:437–42. <https://doi.org/10.1016/j.nmd.2020.05.001>.
- [26] Doorenweerd N, Straathof CS, Dumas EM, Spitali P, Ginjaar IB, Wokke BH, et al. Reduced cerebral gray matter and altered white matter in boys with Duchenne muscular dystrophy. *Ann Neurol* 2014;76:403–11. <https://doi.org/10.1002/ana.24222>.
- [27] Anderson JL, Head SI, Rae C, Morley JW. Brain function in Duchenne muscular dystrophy. *Brain J Neurol* 2002;125:4–13. <https://doi.org/10.1093/brain/awf012>.
- [28] Jagadha V, Becker LE. Brain morphology in Duchenne muscular dystrophy: A Golgi study. *Pediatr Neurol* 1988;4:87–92. [https://doi.org/10.1016/0887-8994\(88\)90047-1](https://doi.org/10.1016/0887-8994(88)90047-1).
- [29] Yoshioka M, Okuno T, Honda Y, Nakano Y. Central nervous system involvement in progressive muscular dystrophy. *Arch Dis Child* 1980;55:589–94. <https://doi.org/10.1136/adc.55.8.589>.
- [30] Suzuki Y, Higuchi S, Aida I, Nakajima T, Nakada T. Abnormal distribution of GABAA receptors in brain of duchenne muscular dystrophy patients. *Muscle Nerve* 2017;55:591–5. <https://doi.org/10.1002/mus.25383>.
- [31] Bagdatlioglu E, Porcari P, Grealley E, Blamire AM, Straub VW. Cognitive impairment appears progressive in the mdx mouse. *Neuromuscul Disord* 2020;30:368–88. <https://doi.org/10.1016/j.nmd.2020.02.018>.
- [32] Naidoo M, Anthony K. Dystrophin Dp71 and the Neuropathophysiology of Duchenne Muscular Dystrophy. *Mol Neurobiol* 2020;57:1748–67. <https://doi.org/10.1007/s12035-019-01845-w>.
- [33] Blake DJ, Weir A, Newey SE, Davies KE. Function and genetics of dystrophin and dystrophin-related proteins in muscle. *Physiol Rev* 2002;82:291–329. <https://doi.org/10.1152/physrev.00028.2001>.

- [34] Gao Q, McNally EM. The Dystrophin Complex: structure, function and implications for therapy. *Compr Physiol* 2015;5:1223–39. <https://doi.org/10.1002/cphy.c140048>.
- [35] Kamdar F, Garry DJ. Dystrophin-Deficient Cardiomyopathy. *J Am Coll Cardiol* 2016;67:2533–46. <https://doi.org/10.1016/j.jacc.2016.02.081>.
- [36] Constantin B. Dystrophin complex functions as a scaffold for signalling proteins. *Biochim Biophys Acta BBA - Biomembr* 2014;1838:635–42. <https://doi.org/10.1016/j.bbamem.2013.08.023>.
- [37] Johnstone VPA, Viola HM, Hool LC. Dystrophic Cardiomyopathy-Potential Role of Calcium in Pathogenesis, Treatment and Novel Therapies. *Genes* 2017;8. <https://doi.org/10.3390/genes8040108>.
- [38] Nitahara-Kasahara Y, Hayashita-Kinoh H, Chiyo T, Nishiyama A, Okada H, Takeda S, et al. Dystrophic mdx mice develop severe cardiac and respiratory dysfunction following genetic ablation of the anti-inflammatory cytokine IL-10. *Hum Mol Genet* 2014;23:3990–4000. <https://doi.org/10.1093/hmg/ddu113>.
- [39] Shirokova N, Niggli E. Cardiac Phenotype of Duchenne Muscular Dystrophy: Insights from Cellular Studies. *J Mol Cell Cardiol* 2013;58:217–24. <https://doi.org/10.1016/j.yjmcc.2012.12.009>.
- [40] Williams IA, Allen DG. Intracellular calcium handling in ventricular myocytes from mdx mice. *Am J Physiol Heart Circ Physiol* 2007;292:H846-855. <https://doi.org/10.1152/ajpheart.00688.2006>.
- [41] Whitehead NP, Yeung EW, Allen DG. Muscle damage in mdx (dystrophic) mice: role of calcium and reactive oxygen species. *Clin Exp Pharmacol Physiol* 2006;33:657–62. <https://doi.org/10.1111/j.1440-1681.2006.04394.x>.
- [42] Deconinck N, Dan B. Pathophysiology of duchenne muscular dystrophy: current hypotheses. *Pediatr Neurol* 2007;36:1–7. <https://doi.org/10.1016/j.pediatrneurol.2006.09.016>.
- [43] Valen G, Yan Z, Hansson GK. Nuclear factor kappa-B and the heart. *J Am Coll Cardiol* 2001;38:307–14. [https://doi.org/10.1016/S0735-1097\(01\)01377-8](https://doi.org/10.1016/S0735-1097(01)01377-8).
- [44] Williams IA, Allen DG. The role of reactive oxygen species in the hearts of dystrophin-deficient mdx mice. *Am J Physiol-Heart Circ Physiol* 2007;293:H1969–77. <https://doi.org/10.1152/ajpheart.00489.2007>.
- [45] Wasala NB, Yue Y, Vance J, Duan D. Uniform low-level dystrophin expression in the heart partially preserved cardiac function in an aged mouse model of Duchenne cardiomyopathy. *J Mol Cell Cardiol* 2017;102:45–52. <https://doi.org/10.1016/j.yjmcc.2016.11.011>.

- [46] van der Velden J, Papp Z, Zaremba R, Boontje NM, de Jong JW, Owen VJ, et al. Increased Ca^{2+} -sensitivity of the contractile apparatus in end-stage human heart failure results from altered phosphorylation of contractile proteins. *Cardiovasc Res* 2003;57:37–47. [https://doi.org/10.1016/s0008-6363\(02\)00606-5](https://doi.org/10.1016/s0008-6363(02)00606-5).
- [47] Rando TA. Role of nitric oxide in the pathogenesis of muscular dystrophies: a “two hit” hypothesis of the cause of muscle necrosis. *Microsc Res Tech* 2001;55:223–35. <https://doi.org/10.1002/jemt.1172>.
- [48] Brenman JE, Chao DS, Xia H, Aldape K, Brecht DS. Nitric oxide synthase complexed with dystrophin and absent from skeletal muscle sarcolemma in Duchenne muscular dystrophy. *Cell* 1995;82:743–52. [https://doi.org/10.1016/0092-8674\(95\)90471-9](https://doi.org/10.1016/0092-8674(95)90471-9).
- [49] Swirski FK, Nahrendorf M. Leukocyte behavior in atherosclerosis, myocardial infarction, and heart failure. *Science* 2013;339:161–6. <https://doi.org/10.1126/science.1230719>.
- [50] Lidov HG, Byers TJ, Watkins SC, Kunkel LM. Localization of dystrophin to postsynaptic regions of central nervous system cortical neurons. *Nature* 1990;348:725–8. <https://doi.org/10.1038/348725a0>.
- [51] Taylor PJ, Betts GA, Maroulis S, Gilissen C, Pedersen RL, Mowat DR, et al. Dystrophin Gene Mutation Location and the Risk of Cognitive Impairment in Duchenne Muscular Dystrophy. *PLOS ONE* 2010;5:e8803. <https://doi.org/10.1371/journal.pone.0008803>.
- [52] Collinson N, Kuenzi FM, Jarolimek W, Maubach KA, Cothliff R, Sur C, et al. Enhanced learning and memory and altered GABAergic synaptic transmission in mice lacking the alpha 5 subunit of the GABAA receptor. *J Neurosci Off J Soc Neurosci* 2002;22:5572–80. <https://doi.org/20026436>.
- [53] Knuesel I, Mastrocola M, Zuellig RA, Bornhauser B, Schaub MC, Fritschy J-M. Altered synaptic clustering of GABAA receptors in mice lacking dystrophin (mdx mice). *Eur J Neurosci* 1999;11:4457–62. <https://doi.org/10.1046/j.1460-9568.1999.00887.x>.
- [54] Rae MG, O’Malley D. Cognitive dysfunction in Duchenne muscular dystrophy: a possible role for neuromodulatory immune molecules. *J Neurophysiol* 2016;116:1304–15. <https://doi.org/10.1152/jn.00248.2016>.
- [55] Waite A, Brown SC, Blake DJ. The dystrophin–glycoprotein complex in brain development and disease. *Trends Neurosci* 2012;35:487–96. <https://doi.org/10.1016/j.tins.2012.04.004>.
- [56] Haenggi T, Soontornmalai A, Schaub MC, Fritschy J-M. The role of utrophin and Dp71 for assembly of different dystrophin-associated protein complexes (DPCS)

- in the choroid plexus and microvasculature of the brain. *Neuroscience* 2004;129:403–13. <https://doi.org/10.1016/j.neuroscience.2004.06.079>.
- [57] Nicchia GP, Nico B, Camassa LMA, Mola MG, Loh N, Dermietzel R, et al. The role of aquaporin-4 in the blood–brain barrier development and integrity: Studies in animal and cell culture models. *Neuroscience* 2004;129:935–44. <https://doi.org/10.1016/j.neuroscience.2004.07.055>.
- [58] Nico B, Frigeri A, Nicchia GP, Corsi P, Ribatti D, Quondamatteo F, et al. Severe alterations of endothelial and glial cells in the blood-brain barrier of dystrophic mdx mice. *Glia* 2003;42:235–51. <https://doi.org/10.1002/glia.10216>.
- [59] Goodnough CL, Gao Y, Li X, Qutaish MQ, Goodnough LH, Molter J, et al. Lack of dystrophin results in abnormal cerebral diffusion and perfusion in vivo. *NeuroImage* 2014;102:809–16. <https://doi.org/10.1016/j.neuroimage.2014.08.053>.
- [60] Sweeney MD, Sagare AP, Zlokovic BV. Blood–brain barrier breakdown in Alzheimer’s disease and other neurodegenerative disorders. *Nat Rev Neurol* 2018;14:133–50. <https://doi.org/10.1038/nrneurol.2017.188>.
- [61] Fiorentino M, Sapone A, Senger S, Camhi SS, Kadzielski SM, Buie TM, et al. Blood–brain barrier and intestinal epithelial barrier alterations in autism spectrum disorders. *Mol Autism* 2016;7:49. <https://doi.org/10.1186/s13229-016-0110-z>.
- [62] Marchi N, Granata T, Ghosh C, Janigro D. Blood–brain barrier dysfunction and epilepsy: Pathophysiologic role and therapeutic approaches. *Epilepsia* 2012;53:1877–86. <https://doi.org/10.1111/j.1528-1167.2012.03637.x>.
- [63] Stephenson KA, Rae MG, O’Malley D. Interleukin-6: A neuro-active cytokine contributing to cognitive impairment in Duchenne muscular dystrophy? *Cytokine* 2020;133:155134. <https://doi.org/10.1016/j.cyto.2020.155134>.
- [64] Comim CM, Ventura L, Freiberger V, Dias P, Bragagnolo D, Dutra ML, et al. Neurocognitive Impairment in mdx Mice. *Mol Neurobiol* 2019;56:7608–16. <https://doi.org/10.1007/s12035-019-1573-7>.
- [65] Wehling M, Spencer MJ, Tidball JG. A nitric oxide synthase transgene ameliorates muscular dystrophy in mdx mice. *J Cell Biol* 2001;155:123–32. <https://doi.org/10.1083/jcb.200105110>.
- [66] Bachiller S, Jiménez-Ferrer I, Paulus A, Yang Y, Swanberg M, Deierborg T, et al. Microglia in Neurological Diseases: A Road Map to Brain-Disease Dependent-Inflammatory Response. *Front Cell Neurosci* 2018;12. <https://doi.org/10.3389/fncel.2018.00488>.
- [67] Hansen DV, Hanson JE, Sheng M. Microglia in Alzheimer’s disease. *J Cell Biol* 2018;217:459–72. <https://doi.org/10.1083/jcb.201709069>.

- [68] Giannoudis PV, Hildebrand F, Pape HC. Inflammatory serum markers in patients with multiple trauma. Can they predict outcome? *J Bone Joint Surg Br* 2004;86:313–23. <https://doi.org/10.1302/0301-620x.86b3.15035>.
- [69] Irimia D, Wang X. Inflammation-on-a-chip: probing the immune system ex vivo. *Trends Biotechnol* 2018;36:923–37. <https://doi.org/10.1016/j.tibtech.2018.03.011>.
- [70] Kany S, Vollrath JT, Relja B. Cytokines in Inflammatory Disease. *Int J Mol Sci* 2019;20. <https://doi.org/10.3390/ijms20236008>.
- [71] Blake GJ, Ridker PM. Inflammatory bio-markers and cardiovascular risk prediction. *J Intern Med* 2002;252:283–94. <https://doi.org/10.1046/j.1365-2796.2002.01019.x>.
- [72] Ballantyne CM, Hoogeveen RC, Bang H, Coresh J, Folsom AR, Chambless LE, et al. Lipoprotein-associated phospholipase A2, high-sensitivity C-reactive protein, and risk for incident ischemic stroke in middle-aged men and women in the Atherosclerosis Risk in Communities (ARIC) study. *Arch Intern Med* 2005;165:2479–84. <https://doi.org/10.1001/archinte.165.21.2479>.
- [73] Jain S, Gautam V, Naseem S. Acute-phase proteins: As diagnostic tool. *J Pharm Bioallied Sci* 2011;3:118–27. <https://doi.org/10.4103/0975-7406.76489>.
- [74] Wang S, Yin P, Quan C, Khan K, Wang G, Wang L, et al. Evaluating the Use of Serum Inflammatory Markers for Preoperative Diagnosis of Infection in Patients with Nonunions. *BioMed Res Int* 2017;2017. <https://doi.org/10.1155/2017/9146317>.
- [75] Cunningham KS, Veinot JP, Butany J. An approach to endomyocardial biopsy interpretation. *J Clin Pathol* 2006;59:121–9. <https://doi.org/10.1136/jcp.2005.026443>.
- [76] Das MK, Chakraborty T. Chapter 3 - Molecular Diagnosis of CNS Viral Infections. In: Kon K, Rai M, editors. *Microbiol. Cent. Nerv. Syst. Infect.*, vol. 3, Academic Press; 2018, p. 45–59. <https://doi.org/10.1016/B978-0-12-813806-9.00003-2>.
- [77] Gault EW. The value and limitations of biopsy examinations. *Aust N Z J Surg* 1966;35:170–6. <https://doi.org/10.1111/j.1445-2197.1966.tb06054.x>.
- [78] Quarantelli M. MRI/MRS in neuroinflammation: methodology and applications. *Clin Transl Imaging* 2015;3:475–89. <https://doi.org/10.1007/s40336-015-0142-y>.
- [79] Magrath P, Maforo N, Renella P, Nelson SF, Halnon N, Ennis DB. Cardiac MRI biomarkers for Duchenne muscular dystrophy. *Biomark Med* 2018;12:1271–89. <https://doi.org/10.2217/bmm-2018-0125>.

- [80] Willcocks R, Arpan I, Forbes S, Lott D, Senesac C, Senesac E, et al. Longitudinal measurements of MRI-T2 in boys with Duchenne muscular dystrophy: Effects of age and disease progression. *Neuromuscul Disord* 2014;24:393–401. <https://doi.org/10.1016/j.nmd.2013.12.012>.
- [81] Johnston JH, Kim HK, Merrow AC, Laor T, Serai S, Horn PS, et al. Quantitative Skeletal Muscle MRI: Part 1, Derived T2 Fat Map in Differentiation Between Boys With Duchenne Muscular Dystrophy and Healthy Boys. *Am J Roentgenol* 2015;205:W207–15. <https://doi.org/10.2214/AJR.14.13754>.
- [82] Mankoff DA. A definition of molecular imaging. *J Nucl Med Off Publ Soc Nucl Med* 2007;48:18N, 21N.
- [83] MacRitchie N, Frleta-Gilchrist M, Sugiyama A, Lawton T, McInnes IB, Maffia P. Molecular imaging of inflammation - Current and emerging technologies for diagnosis and treatment. *Pharmacol Ther* 2020;211:107550. <https://doi.org/10.1016/j.pharmthera.2020.107550>.
- [84] Glaudemans AWJM, de Vries EFJ, Galli F, Dierckx RAJO, Slart RHJA, Signore A. The use of (18)F-FDG-PET/CT for diagnosis and treatment monitoring of inflammatory and infectious diseases. *Clin Dev Immunol* 2013;2013:623036. <https://doi.org/10.1155/2013/623036>.
- [85] James OG, Christensen JD, Wong TZ, Borges-Neto S, Koweek LM. Utility of FDG PET/CT in inflammatory cardiovascular disease. *Radiogr Rev Publ Radiol Soc N Am Inc* 2011;31:1271–86. <https://doi.org/10.1148/rg.315105222>.
- [86] Winkeler A, Boisgard R, Martin A, Tavitian B. Radioisotopic imaging of neuroinflammation. *J Nucl Med Off Publ Soc Nucl Med* 2010;51:1–4. <https://doi.org/10.2967/jnumed.109.065680>.
- [87] Wu C, Li F, Niu G, Chen X. PET Imaging of Inflammation Biomarkers. *Theranostics* 2013;3:448–66. <https://doi.org/10.7150/thno.6592>.
- [88] Rosenbaum SJ, Lind T, Antoch G, Bockisch A. False-positive FDG PET uptake--the role of PET/CT. *Eur Radiol* 2006;16:1054–65. <https://doi.org/10.1007/s00330-005-0088-y>.
- [89] Carter K, Kotlyarov E. Common causes of false positive F18 FDG PET/CT scans in oncology. *Braz Arch Biol Technol - BRAZ ARCH BIOL TECHNOL* 2007;50. <https://doi.org/10.1590/S1516-89132007000600004>.
- [90] Giatzakis C, Papadopoulos V. Differential utilization of the promoter of peripheral-type benzodiazepine receptor by steroidogenic versus nonsteroidogenic cell lines and the role of Sp1 and Sp3 in the regulation of basal activity. *Endocrinology* 2004;145:1113–23. <https://doi.org/10.1210/en.2003-1330>.

- [91] Chen M-K, Guilarte TR. Translocator protein 18 kDa (TSPO): Molecular sensor of brain injury and repair. *Pharmacol Ther* 2008;118:1–17. <https://doi.org/10.1016/j.pharmthera.2007.12.004>.
- [92] Wilms H, Claasen J, Röhl C, Sievers J, Deuschl G, Lucius R. Involvement of benzodiazepine receptors in neuroinflammatory and neurodegenerative diseases: evidence from activated microglial cells in vitro. *Neurobiol Dis* 2003;14:417–24. <https://doi.org/10.1016/j.nbd.2003.07.002>.
- [93] Gerhard A, Neumaier B, Elitok E, Glatting G, Ries V, Tomczak R, et al. In vivo imaging of activated microglia using [11C]PK11195 and positron emission tomography in patients after ischemic stroke. *Neuroreport* 2000;11:2957–60. <https://doi.org/10.1097/00001756-200009110-00025>.
- [94] Thackeray JT, Hupe HC, Wang Y, Bankstahl JP, Berding G, Ross TL, et al. Myocardial Inflammation Predicts Remodeling and Neuroinflammation After Myocardial Infarction. *J Am Coll Cardiol* 2018;71:263–75. <https://doi.org/10.1016/j.jacc.2017.11.024>.
- [95] Venneti S, Lopresti BJ, Wang G, Bissel SJ, Mathis CA, Meltzer CC, et al. PET imaging of brain macrophages using the peripheral benzodiazepine receptor in a macaque model of neuroAIDS. *J Clin Invest* 2004;113:981–9. <https://doi.org/10.1172/JCI200420227>.
- [96] Hammoud DA. Molecular Imaging of Inflammation: Current Status. *J Nucl Med Off Publ Soc Nucl Med* 2016;57:1161–5. <https://doi.org/10.2967/jnumed.115.161182>.
- [97] Kim GR, Paeng JC, Jung JH, Moon BS, Lopalco A, Denora N, et al. Assessment of TSPO in a Rat Experimental Autoimmune Myocarditis Model: A Comparison Study between [18F]Fluoromethyl-PBR28 and [18F]CB251. *Int J Mol Sci* 2018;19. <https://doi.org/10.3390/ijms19010276>.
- [98] Cuhlmann S, Gsell W, Van der Heiden K, Habib J, Tremoleda JL, Khalil M, et al. In vivo mapping of vascular inflammation using the translocator protein tracer 18F-FEDAA1106. *Mol Imaging* 2014;13. <https://doi.org/10.2310/7290.2014.00014>.
- [99] Hellberg S, Silvola JMU, Kiugel M, Liljenbäck H, Savisto N, Li X-G, et al. 18-kDa translocator protein ligand 18F-FEMPA: Biodistribution and uptake into atherosclerotic plaques in mice. *J Nucl Cardiol Off Publ Am Soc Nucl Cardiol* 2017;24:862–71. <https://doi.org/10.1007/s12350-016-0527-y>.
- [100] Hashimoto K, Inoue O, Suzuki K, Yamasaki T, Kojima M. Synthesis and evaluation of 11C-PK 11195 for in vivo study of peripheral-type benzodiazepine receptors using positron emission tomography. *Ann Nucl Med* 1989;3:63–71. <https://doi.org/10.1007/BF03164587>.

- [101] Wilson AA, Garcia A, Parkes J, McCormick P, Stephenson KA, Houle S, et al. Radiosynthesis and initial evaluation of [18F]-FEPPA for PET imaging of peripheral benzodiazepine receptors. *Nucl Med Biol* 2008;35:305–14. <https://doi.org/10.1016/j.nucmedbio.2007.12.009>.
- [102] Kannan S, Balakrishnan B, Muzik O, Romero R, Chugani D. PET Imaging of Neuroinflammation. *J Child Neurol* 2009;24. <https://doi.org/10.1177/0883073809338063>.
- [103] Pugliese F, Gaemperli O, Kinderlerer AR, Lamare F, Shalhoub J, Davies AH, et al. Imaging of vascular inflammation with [11C]-PK11195 and positron emission tomography/computed tomography angiography. *J Am Coll Cardiol* 2010;56:653–61. <https://doi.org/10.1016/j.jacc.2010.02.063>.
- [104] Chauveau F, Boutin H, Van Camp N, Dollé F, Tavitian B. Nuclear imaging of neuroinflammation: a comprehensive review of [11C]PK11195 challengers. *Eur J Nucl Med Mol Imaging* 2008;35:2304–19. <https://doi.org/10.1007/s00259-008-0908-9>.
- [105] Zanotti-Fregonara P, Pascual B, Rizzo G, Yu M, Pal N, Beers D, et al. Head-to-head comparison of 11C-PBR28 and 18F-GE180 for the quantification of TSPO in the human brain. *J Nucl Med* 2018;jnumed.117.203109. <https://doi.org/10.2967/jnumed.117.203109>.
- [106] Alam MdM, Lee J, Lee S-Y. Recent Progress in the Development of TSPO PET Ligands for Neuroinflammation Imaging in Neurological Diseases. *Nucl Med Mol Imaging* 2017;51:283–96. <https://doi.org/10.1007/s13139-017-0475-8>.
- [107] McGreevy JW, Hakim CH, McIntosh MA, Duan D. Animal models of Duchenne muscular dystrophy: from basic mechanisms to gene therapy. *Dis Model Mech* 2015;8:195–213. <https://doi.org/10.1242/dmm.018424>.
- [108] Ahmad N, Welch I, Grange R, Hadway J, Dhanvantari S, Hill D, et al. Use of imaging biomarkers to assess perfusion and glucose metabolism in the skeletal muscle of dystrophic mice. *BMC Musculoskelet Disord* 2011;12:127. <https://doi.org/10.1186/1471-2474-12-127>.
- [109] Vaillend C, Billard J-M, Laroche S. Impaired long-term spatial and recognition memory and enhanced CA1 hippocampal LTP in the dystrophin-deficient Dmdmdx mouse. *Neurobiol Dis* 2004;17:10–20. <https://doi.org/10.1016/j.nbd.2004.05.004>.
- [110] Muntoni F, Mateddu A, Serra G. Passive avoidance behaviour deficit in the mdx mouse. *Neuromuscul Disord* 1991;1:121–3. [https://doi.org/10.1016/0960-8966\(91\)90059-2](https://doi.org/10.1016/0960-8966(91)90059-2).

- [111] Vaillend C, Ungerer A. Behavioral characterization of mdx3cv mice deficient in C-terminal dystrophins. *Neuromuscul Disord NMD* 1999;9:296–304. [https://doi.org/10.1016/s0960-8966\(99\)00029-2](https://doi.org/10.1016/s0960-8966(99)00029-2).
- [112] Yucel N, Chang AC, Day JW, Rosenthal N, Blau HM. Humanizing the mdx mouse model of DMD: the long and the short of it. *NPJ Regen Med* 2018;3:4. <https://doi.org/10.1038/s41536-018-0045-4>.
- [113] Tinsley JM, Potter AC, Phelps SR, Fisher R, Trickett JI, Davies KE. Amelioration of the dystrophic phenotype of mdx mice using a truncated utrophin transgene. *Nature* 1996;384:349–53. <https://doi.org/10.1038/384349a0>.
- [114] Gutpell KM, Hrinivich WT, Hoffman LM. Skeletal Muscle Fibrosis in the mdx/utrn+/- Mouse Validates Its Suitability as a Murine Model of Duchenne Muscular Dystrophy. *PLoS ONE* 2015;10. <https://doi.org/10.1371/journal.pone.0117306>.
- [115] Hainsey TA, Senapati S, Kuhn DE, Rafael JA. Cardiomyopathic features associated with muscular dystrophy are independent of dystrophin absence in cardiovascular. *Neuromuscul Disord NMD* 2003;13:294–302. [https://doi.org/10.1016/s0960-8966\(02\)00286-9](https://doi.org/10.1016/s0960-8966(02)00286-9).
- [116] Meng Y, Tian M, Yin S, Lai S, Zhou Y, Chen J, et al. Downregulation of TSPO expression inhibits oxidative stress and maintains mitochondrial homeostasis in cardiomyocytes subjected to anoxia/reoxygenation injury. *Biomed Pharmacother* 2020;121:109588. <https://doi.org/10.1016/j.biopha.2019.109588>.

Chapter 2

2 *In-vivo* imaging of cardiac and neuroinflammation in Duchenne muscular dystrophy mice: a [¹⁸F]FEPPA PET study

This chapter has been adapted from the following manuscript:

Tang JM, McClennan A, Liu L, Hadway J, Ronald J, Hicks JW, Hoffman L, Anazodo UC. *In-vivo* imaging of cardiac and neuroinflammation in Duchenne muscular dystrophy: a [¹⁸F]FEPPA PET study. Submitted to Neuromuscul Disord in August 2020. Under Review. Manuscript ID: NWD-S-20-00539.

2.1 Introduction

Duchenne muscular dystrophy (DMD) is a progressive neuromuscular degenerative disease, affecting approximately 1 in 3600 live male births worldwide. Individuals with DMD are unable to produce functional Dystrophin protein which is found systemically across various tissues, notably in skeletal and cardiac muscle, and neurons in the central nervous system (CNS). As a result, DMD is clinically characterized by progressive skeletal and cardiac muscle degeneration along with cognitive impairment [1–3]. These multi-organ degenerations are exacerbated by fibrosis, ischemia, and chronic inflammation until an early death from cardiac or respiratory complications [4–6]. Although there is still no cure for DMD, recent advancements in experimental therapies have prolonged both ambulation and life expectancy, as fatalities previously expected by age 15–20, are now often observed at approximately age 30–40 [5,7].

Due to the improved management of skeletal and respiratory dysfunctions, more patients are now surviving long enough for the emergence of heart failure and cognitive impairment associated with the later stages of the disease. In fact, more than 90% of DMD patients over the age of 18 show signs of cardiac involvement, with nearly 60% of

DMD patients dying from cardiac complications by age 19 [8,9]. Likewise 20–50% of males demonstrate some form of cognitive weakness which remain, and in some cases, exacerbates as they get older (~age 30) [10–12]. Thus, with increased longevity in DMD patients, the clinical relevance of heart disease and cognitive impairment in DMD is becoming more apparent, increasing the need for the better understanding of both dystrophic cardiac and neurological involvement. Currently, it is known that the dystrophin loss in cardiac muscles leads to membrane integrity deterioration of striated cardiac muscle fibers and impaired regulation of intracellular calcium levels. As with skeletal muscle, it is suspected that this membrane instability and associated intracellular calcium influx initiate the pathological cycle of chronic inflammation, fibrosis, necrosis, leading to damage in regions of high contractility and movement (e.g. left ventricle). The loss of viable myocardium leads to further fibrosis, and the clinical emergence of cardiomyopathy and eventually heart failure [5,6,13–15].

The brain is a far less studied organ in DMD, but dystrophin also plays a role in brain development and aging. The lack of intrinsic dystrophin gene products within CNS—namely Dp427, Dp140, and Dp71—are thought to contribute to cognitive weakness by contributing to a series of functional and morphological abnormalities within the dystrophic brain [2,3,16]. However, the underlying mechanisms are not well understood. Cognitive and behavioural symptoms usually manifest in the form of lowered intelligence quotient (IQ) scores, learning difficulties, memory deficits, and higher incidences of neuropsychiatric disorders [16]. Recent investigations also report the delayed emergence of cerebral infarcts and progressive cognitive decline within older DMD subjects, leading to the possible paradigm of neurodegeneration in the later stages of disease progression [10,12,17].

While mechanical injury and membrane defects are thought to be proximate causes of DMD, secondary mechanisms encompassing chronic inflammation, fibrosis, and ischemia also contribute to the defective physiology. Indeed, inflammatory cell infiltration is strongly associated with DMD as it is thought to exacerbate symptoms and promote muscular degeneration [4,6,14]. We recently demonstrated that the degree of inflammatory cell infiltration is correlated with disease progression within DMD murine

models [18]. While there is growing evidence that inflammation may be an inciting factor in skeletal muscle degeneration and the development of cardiomyopathy in DMD, the role of inflammation within the dystrophic brain in DMD is relatively unexplored—despite neuroinflammation being a prime proponent to several pediatric and adult neurodegenerative disorders [4,19–21]. To the best of our knowledge, immune cell infiltration has yet to be demonstrated within neither the DMD patient nor animal model brain. However, in brain tissue from the *mdx* murine model of DMD, heightened levels of pro-inflammatory cytokines in interleukin (IL)-1 β and Tumor Necrosis Factor (TNF)- α were found and several cognitive deficits were observed [22]. Other neurological diseases are also associated with increased levels of TNF- α and IL-1 β [23]. Thus, considering the well-known consequences of unchecked inflammation potentially leading to cardiac and neurodegeneration, there is an unmet need to better understand the role of inflammation in multi-organ degeneration, as it may lead to the subsequent development of effective therapeutic strategies that targets multiple tissues systems especially brain and heart resilience in DMD patients.

Recent advancements in non-invasive molecular imaging techniques for assessing inflammatory load have already inspired interest in understanding the role of inflammation in multi-organ degeneration in several disease systems. In particular, Thackeray et al. [24] demonstrated evidence of concomitant inflammation in both the hearts and brains of ischemic heart disease mice and patients using positron emission tomography (PET) imaging targeting mitochondrial translocator protein (TSPO). TSPOs are highly expressed on activated microglia and macrophages [25]. Thus, this exploratory study sought to explore the capacity of TSPO-PET imaging in assessing in-vivo inflammatory involvement in DMD in the heart and brain as well as across several organs. Specifically, we used [^{18}F]-N-(2-(2-fluoroethoxy)benzyl)-N-(4-phenoxy-pyridin-3-yl)acetamide ([^{18}F]FEPPA), a second-generation TSPO tracer, to assess cardiac and neural inflammation in DMD [25]. We hypothesized that mice with DMD will have increased inflammation levels in dystrophic cardiac and neural tissues, exhibited as heightened TSPO-PET signal and correlative histological TSPO expression.

2.2 Materials and Methods

The study was conducted at Lawson Health Research Institute at St. Joseph's Health Care in London, Ontario. All animal protocols were approved by the Animal Use Subcommittee at Western University and were conducted in accordance with guidelines set by the Canadian Council on Animal Care (CCAC).

2.2.1 Study Population

Breeding pairs of wild-type (C57BL/10) and functional dystrophin-deficient *mdx:utrn*(+/-) (a point mutation in dystrophin gene) mice were purchased from Charles River and Jackson Laboratories (Bar Harbor, ME) [26]. Colonies were maintained under controlled conditions (19-23°C, 12-hour light/dark cycles), and were allowed water and food ad libitum. Two separate groups of eight to ten week old mice were used in this study where the *in-vivo* imaging (n=4-6 mice/genotype) and *ex-vivo* histology cohorts (n=3 mice/genotype) are henceforth to be referred to as the PET and immunohistochemistry (IHC) cohort, respectively.

2.2.2 Small animal PET Imaging Protocol

All PET mice were induced in a chamber with 3% oxygen-balanced isoflurane mixture and then anesthetized with 1.5 – 2%; both mixtures were delivered at a constant rate of 1L/min via a nose cone. After induction, these mice were imaged using a micro-PET scanner (eXplore VISTA, GE Healthcare; Inveon DPET, Siemens). To assess whole-body inflammation accumulation, TSPO-targeted PET images were obtained after [¹⁸F]FEPPA tracer injection. 30 seconds following the start of the scan, a dose of approximately 20 MBq of prepared [¹⁸F]FEPPA in saline (approximately 5µg/kg) was administered via tail vein catheter for dynamic acquisition. Summarily, a 60-minute whole-body dynamic scan in list-mode was acquired using the Inveon system. Upon using the eXplore VISTA scanner, list-mode acquisition was also conducted upon a 60 minute dynamic scan of the head-to-chest region, followed by a 30 minute full-body static scan. Injected dose did not exceed 0.3 mL to ensure proper animal health conditions.

2.2.3 PET Imaging Analysis

For each subject, the dynamic PET list mode data were reconstructed into the following time frames: 12×10 s, 6×30 s, 5×60 s, 5×120 s, 8×300 s using ordered subset expectation maximization (OSEM) algorithm with no scatter and attenuation correction. Data were corrected to injected dose and decay corrected to start of PET scan using in-house MATLAB v2019a scripts (Mathworks, Natick, MA, USA). Standardized Uptake Values (SUV) were generated from PET data 30-60 minutes post-injection in PMOD 3.9 (PMOD Technologies, Zurich, Switzerland). Using manually drawn regions of interest (ROI), mean SUV were calculated for the left ventricle, lung, and whole brain covering 3-4 slices. Left ventricle-to-heart ratio—used to offset lung [^{18}F]FEPPA activity and act as a correlative of cardiac events—was calculated from mean SUV within each animal [27].

2.2.4 Biodistribution and Autoradiography

The mice were sacrificed immediately after imaging through 5% oxygen-balanced isoflurane gas euthanasia followed by cervical dislocation. To preserve tissue anatomy, the mice underwent whole animal perfusion fixation via an intracardiac infusion of 4% paraformaldehyde (Sigma-Aldrich), and then phosphate-buffered saline (PBS) as directed in Gage et al. [28]. The heart and brain were dissected from the subjects. Each heart was bisected twice—once transversely and once along the septum—and each brain were bisected along the central sulcus to ensure that exactly half of each tissue was fixed in 10% Formalin or frozen in Optimal Cutting Temperature solution (VWR) for biodistribution and autoradiography use respectively. Biodistribution was conducted for the heart, brain, thoracic aorta, diaphragm, gastrocnemius, soleus, tibialis anterior, large/small intestines, tibia/fibula, kidney, liver, and lungs; each organ was weighed for quantitative estimation of gamma counts from the ^{18}F conjugate using the ORETC DSPEC50 Spectrometer. Radioactivity obtained from different organs was calculated as the percentage of the injected dose per gram of the tissue (%ID/g) and decay corrected to time of injection. Radioactivity was standardized to the dose injected into each animal. For autoradiography, frozen tissue samples were cryosectioned into a thickness of 20 μm

with a Leica Clinical Cryostat (CM1850, Leica Biosystems, Wetzlar, Germany). Autoradiographic images of the heart, brain, thoracic aorta, diaphragm, gastrocnemius, tibialis anterior, kidney and liver were acquired for 12 h using a digital autoradiography system (JTV-18-0008, AI4R, Nantes, France) fitted with a HEEL positron holder.

2.2.5 Histology

2.2.5.1 Tissue Preparation

To supplement data from acute imaging for immunohistochemistry analysis, a cohort of mice were sacrificed through cervical dislocation following CO₂ gas euthanasia without PET imaging. The heart and brain were dissected and fixed in 10% formalin for 24–48 h. These tissues were processed for immunohistochemistry by being embedded in paraffin by the Molecular Pathology facility (Robarts Research Institute, London, ON) and cut into 10 µm thick sections. Care was taken to ensure that the tissues were embedded in the same orientation within each block.

2.2.5.2 Immunohistochemistry Protocol

Following a modified protocol based on Abcam standards, tissue sections were deparaffinized and rehydrated in a series of xylene and ethanol washes prior to heat-mediated antigen retrieval in a citrate buffer for 30 minutes. Slides were then cooled slowly to room temperature, and Background Sniper (Biocare Medical) was applied for 8 minutes to reduce nonspecific background staining. Sections were incubated overnight at 4 °C with either primary anti-PBR (1:200, Abcam), primary anti- α -SMA (1:500, Abcam), or no antibodies—the latter acting as the positive and negative control. All antibodies were diluted in 1% bovine serum albumin (BSA) PBS. Following thorough washing with 1 × PBS, Alexafluor IgG (Life Technologies, 1:500) secondary antibodies were used to visualize the primary antibodies: anti-PBR sections were incubated with 594 Goat anti-rabbit IgG, and anti- α -SMA sections with 488 Goat anti-mouse IgG for 2 h at room temperature. For heart tissue, a solution of Cu₂SO₄•5H₂O was applied thereafter to prevent red blood cell autofluorescence. Additional 1 × PBS washes and an immersion in 0.1% Sudan Black B was performed to quench autofluorescence in both heart and brain

tissue sections. Lastly, ProLong Gold anti-fade with DAPI (Life Technologies) was added to all sections to visualize the nuclei and to mount the coverslips onto glass slides.

2.2.5.3 Microscopy and Image Analysis

Fluorescent images were acquired on an epifluorescence microscope (Nikon Eclipse Ts2R) using NIS Elements Microscope Image Software. Non-overlapping fields of view at 60x magnification were taken for each tissue section (n=5-10 images/slide). Quantitative assessment of TSPO fluorescent signal in both wild-type and *mdx:utrn*(+/-) (henceforth named DMD) subjects—while minimizing image exposure and autofluorescence (i.e. background signal)—was performed using an in-house semi-automatic grey scale thresholding protocol in ImageJ (LOCI, Wisconsin, USA) with FIJI package v2.0.0 [29].

2.2.6 Statistical Analysis

Analyses were performed using RStudio v1.0.136 (Boston, MA, USA) or SPSS 26 (IBM, Armonk, NY, USA) software. Data results are expressed as mean \pm standard error (SE). Comparisons between groups were performed using Welch's two-tailed t-test. No statistical analyses were conducted on autoradiography and biodistribution data due to low sample sizes. Negative biodistribution values were removed from the data set. Pearson correlation coefficients were calculated between [^{18}F]FEPPA left ventricle/whole brain uptake, and myocardium/neural tissue histological TSPO fluorescence intensity. P-values of less than 0.05 were considered significant. Replicate numbers are indicated in the figure legends.

2.3 Results

A total of four DMD and six healthy mice were imaged. Both healthy and DMD mice were both able to take up [^{18}F]FEPPA throughout the entire body—notably binding to our tissues of interest, the heart and brain (Fig. 2.1). Although there were not sufficient tissue samples to measure differences in [^{18}F]FEPPA binding using autoradiography and biodistribution, preliminary results demonstrates [^{18}F]FEPPA activity occurring body-

wide within the heart and brain as well as in several other tissues, such as skeletal muscles, aorta, diaphragm, etc. as shown in Appendix Figure A.1 and Figure A.2.

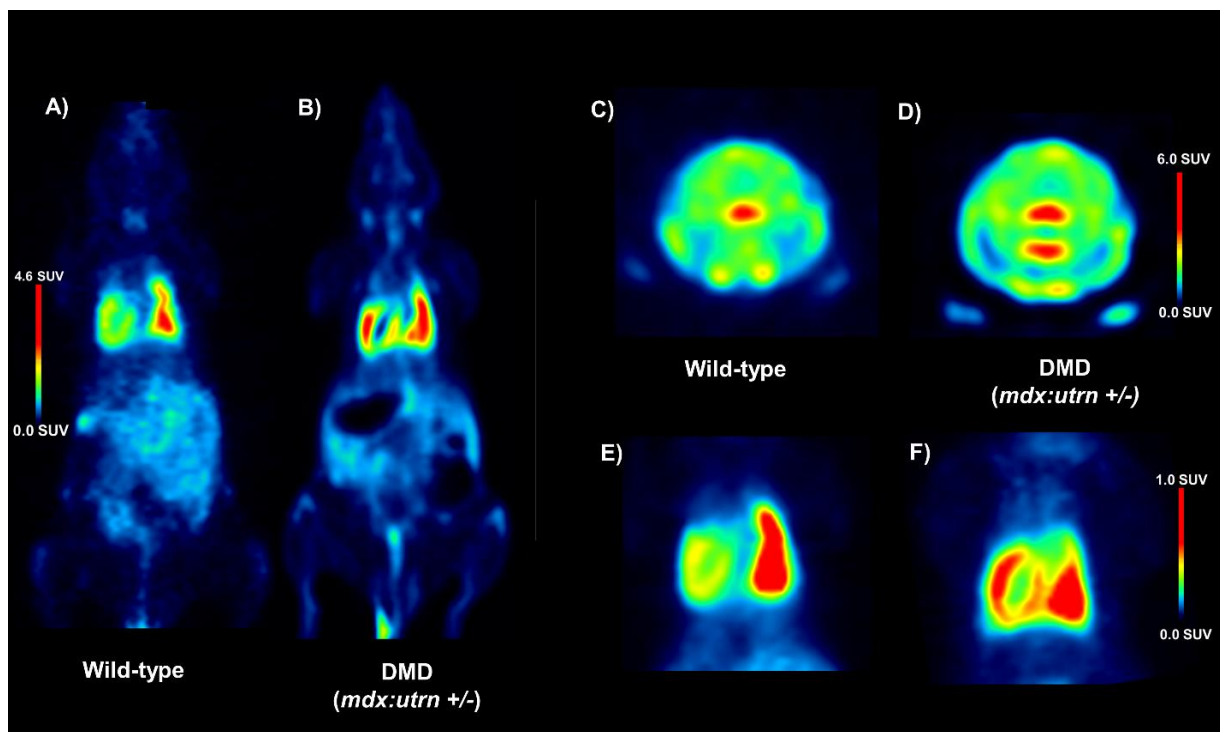


Figure 2.1 [^{18}F]FEPPA SUV images of representative 8-10 week wild-type (A, C, E) and age-matched Duchenne muscular dystrophy (B, D, F) mice. Coronal whole-body (A, B) and heart images (E, F), and axial whole brain slices (C, D) were generated from PET time-activity curves at 30-60 minutes ($n=4-6$ mice/genotype). DMD=Duchenne muscular dystrophy, SUV=Standardized uptake values.

2.3.1 Elevation of *in-vivo* inflammation-targeted radiotracer binding in DMD models

To assess the influence of inflammation on dystrophic cardiac and neural tissue, inflammation was quantified from the [^{18}F]FEPPA PET images as mean SUV. In the thoracic region, left ventricle-to-lung mean SUV ratios indicated that DMD mice had significantly higher [^{18}F]FEPPA uptake (Fig. 2.2; $T_{1,7.62}=2.58$, $P=0.0338$), as these left ventricle-to-lung ratios increased from 0.63 ± 0.10 in healthy mice to 0.99 ± 0.06 in their DMD equivalents. In neural tissue, similar accumulations of inflammatory tracer were

also observed in DMD mice. Healthy brains demonstrated [^{18}F]FEPPA uptake of 0.34 ± 0.08 SUV, while DMD brains experienced 45.4% more uptake at 0.62 ± 0.08 SUV.

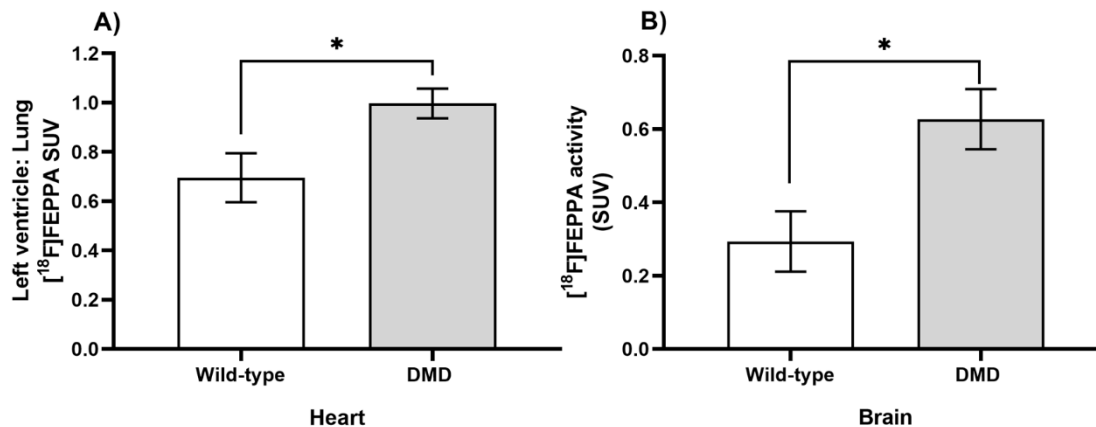


Figure 2.2 Quantified [^{18}F]FEPPA activity in hearts (A) and brains (B) of age-matched DMD and wild-type mice. Standardized uptake values were generated from PET time-activity curves at 30-60 minutes using manually drawn regions of interest (ROIs) segmented for the left ventricle, lung, and whole brain (n=3-4 slices/subject/genotype). Significant differences ($p < 0.05$; indicated by *) were observed between wild-type (white bars) and DMD mice (gray bars) for both left ventricle-to-lung ratio (A) and whole brain (B) SUVs using Welch's two-way t-test. Data are depicted as mean \pm standard error. TSPO = (18kDa) Translocator protein, other abbreviations as described in prior figures.

2.3.2 *Ex-vivo* TSPO signal indicates heightened cardiac and neuroinflammation in DMD

Fluorescence immunostaining of heart and brain slices confirmed the presence of TSPO in age-matched DMD subjects. Although both groups expressed a modest baseline level of TSPO (Fig. 2.3); consistently, DMD mice expressed significantly higher TSPO fluorescence intensity in both cardiac (Fig. 2.4; $T_{1,31,2}=2.35$, $P=0.025$) and neural tissue (Fig. 2.4; $T_{1,69,2}=5.15$, $P < 0.001$). Within cardiac tissue, DMD mice experienced a 63.9% increase in fluorescence intensity when compared to age-matched wild-type mice; as dystrophic hearts demonstrated TSPO fluorescence intensities of 1261.57 ± 307.76 AU compared to those of wild-type mice at 454.59 ± 63.93 AU. Similarly, in neural tissue,

TSPO fluorescence intensity was remarkably 68.3% lower in healthy controls compared to DMD mice. Dystrophic brain tissues displayed fluorescence intensities of 1149.74 ± 148.35 AU, which is lower than the 364.84 ± 73.71 AU observed in wild-type brains. Histological myocardium TSPO signal significantly correlated with [^{18}F]FEPPA uptake in the left ventricle (Fig. 2.5; $r=0.59$, $p=0.037$). This was also observed between neural tissue TSPO fluorescence intensity in histology and *in-vivo* whole brain TSPO-PET tracer SUV values (Fig. 2.5; $r=0.57$, $p=0.042$).

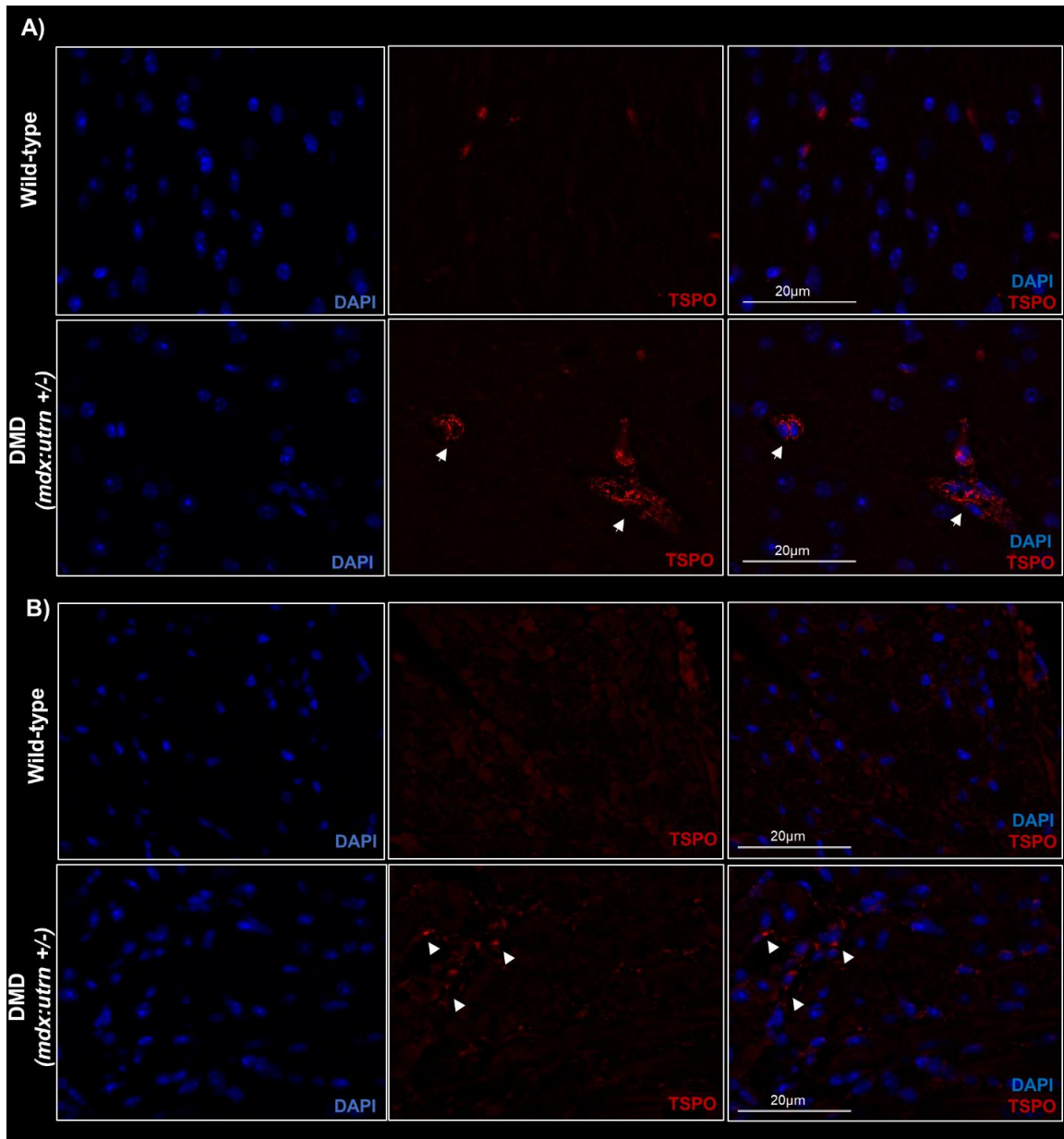


Figure 2.3 *Ex-vivo* histology of TSPO-bound microglial and macrophages in DMD and healthy subjects' cardiac (A) and neural tissues (B). Representative fluorescence immunostained images of microglial and macrophages with TSPO (red) and DAPI (blue) in 8-10 week old subjects depict qualitatively more prevalent TSPO expression in DMD mice. White arrow heads indicate regions of TSPO signal. Scale bar= 20μm. Abbreviations as described in prior figures.

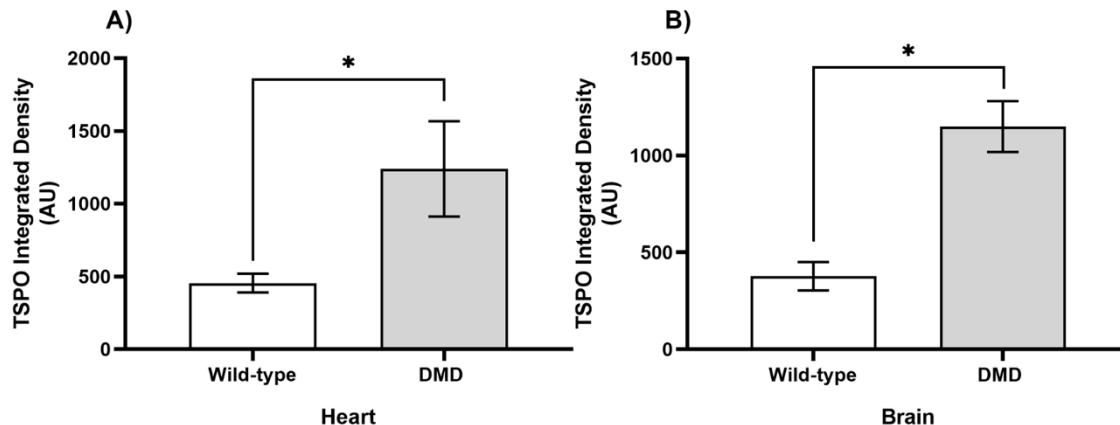


Figure 2.4 Quantified fluorescence immunohistochemical images of microglial and macrophages with TSPO in 8-10 week old DMD and healthy subjects. Data (mean \pm SE) depicts higher TSPO in DMD mice (gray bars) than wild-type controls (white bars) (n=3 mice/genotype). Significant differences (p<0.05), indicated by *, were observed for slices of cardiac (A) and neural (B) tissue when compared using Welch's two-way t-test (n=5-10 images/subject/genotype). AU= arbitrary units. Other abbreviations as described in prior figures.

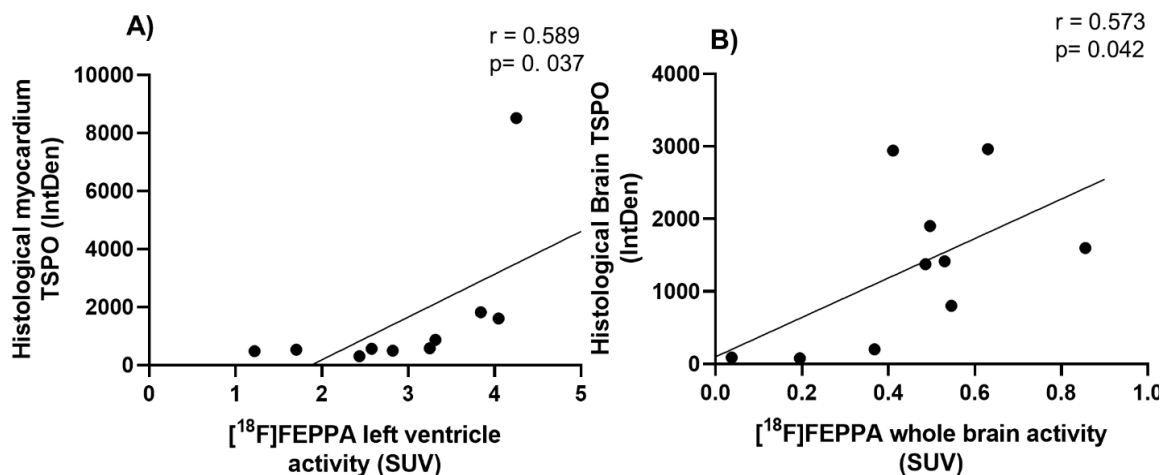


Figure 2.5 Correlation of [18F]FEPPA uptake with histological TSPO fluorescence intensity. Data depicts the significant correlation of the left ventricle (A) or whole brain (B) SUV, with quantified TSPO myocardium or neural tissue fluorescence signal. Pearson product-moment correlation coefficients (r) were calculated on all PET animals (n=10). Significance was considered when p<0.05. Abbreviations as described in prior figures.

2.4 Discussion

The goal of this exploratory study was to evaluate the ability of [^{18}F]FEPPA PET as a tool to assess inflammation *in-vivo* in multiple organs of mice with dystrophic disease. We found dystrophin-deficient mice had elevated [^{18}F]FEPPA uptake in cardiac and neural tissues compared to healthy controls, which mirrored heightened *ex-vivo* TSPO levels in our histological data. These results support our hypothesis that subjects with DMD demonstrate significant inflammation in their heart and brains using TSPO-PET.

To the best of our knowledge, our study is one of the first to observe significantly elevated TSPO-PET in the heart and brains of DMD mice. Interestingly, these increases seem to be occurring body-wide within several other tissues, akin to other diseases linked to chronic inflammation (e.g. atherosclerosis, myocardial infarctions, etc.) [24,30,31]. As such, it is likely that this heightened TSPO activity may be a consequence of activated macrophages and microglia within regions of tissue injury or dysfunction [31]. For example, immunohistostaining of mice one week post-myocardial infarction indicated colocalization of TSPO to CD68+ microglia and cardiac monocytes within the brain cortex and infarcted myocardium respectively [24]. Interestingly, no colocalization was found between TSPO and GFAP-stained astrocytes at that time point. TSPO-tracers were also found to localize to magnetic resonance imaging (MRI)-identified ischemic lesions within ischemic stroke patients, further demonstrating the tracer's feasibility to also map inflammation after incidences of tissue damage [32]. Thus, as DMD pathophysiology is known to be associated with contraction-induced damage and severe immune cell infiltration, it is likely that TSPO is upregulated within regions of injury—manifesting as the displayed [^{18}F]FEPPA tracer uptake within the dystrophic heart and brain. Our preliminary biodistribution and autoradiography observations support these claims, as the TSPO-tracer accumulated notably within regions associated with DMD symptoms (i.e. heart, brain, skeletal muscles, etc.). Although this exploratory study demonstrated the feasibility of [^{18}F]FEPPA PET to assess *in-vivo* inflammation simultaneously within the heart and the brain, our study cannot provide a definite answer to whether [^{18}F]FEPPA PET can demonstrate inflammatory load within other tissues—despite the promising trends—due to the small sample sizes of our autoradiography and biodistribution data. To

answer this question, a study using a larger sample size as well as the quantification of tracer uptake in the other tissues within the PET data is needed.

In contrast to our results, three previous 2-deoxy-2- ^{18}F fluoro-D-glucose (^{18}F FDG) PET studies reported lower mean cardiac SUV and highlighted select neural regions of hypometabolism in DMD canine hearts and patient brains, respectively [33–35]. While ^{18}F FDG can be used as an analogue of inflammation in several neurological and cardiac diseases, it should be noted that these specific studies were focused on investigating the metabolic functionality of dystrophin-deficient tissue regions rather than its associated peripheral inflammation [36,37]. Because of the heart and the brain's disposition as highly metabolically-active organs, there is naturally a higher accumulation of ^{18}F FDG tracer within those regions, which makes it difficult to detect inflammatory infiltrates within either organ without it potentially being obscured by background activity or alterations in myocardial/neuronal function [38,39]. Additionally, a multi-tracer study longitudinally tracking microglial activation and glucose hypometabolism simultaneously in a transgenic mouse model of Alzheimer's disease observed discrepancies between the data trend of the TSPO-tracer ^{18}F GE-180 and ^{18}F FDG [40]. The authors observed progressive increases in ^{18}F GE-180 uptake throughout the entire course of the disease (5-16 months), which differed from the life-course kinetics of ^{18}F FDG which peaked at ~8 months of age before decreasing for the remaining 8 months, suggesting that the incidences of hypometabolism demonstrated within the dementia subjects are occurring much later in life and as disease progressed. Interestingly, this early hypermetabolism may be capturing increased glial activity as it matches the peak of ^{18}F GE-180 at 8 months—indicating the potential early onset of inflammation prior to rampant hypometabolism (and with it, the neurodegenerative symptoms) [41]. Taken together, although prior ^{18}F FDG studies in DMD subjects show known indications of late-life brain and cardiac degeneration/dysfunction, our data highlights the potential role of inflammation in contributing to these metabolic deficiencies within DMD mice. Further longitudinal multi-tracer studies on dystrophic subjects using both ^{18}F FEPPA and ^{18}F FDG would greatly improve our understanding of the time course and interaction of inflammation and glucose hypometabolism onset.

The increased *in-vivo* [¹⁸F]FEPPA activity within the heart of our DMD mice correlated with increases in *ex-vivo* histology, demonstrating that TSPO overexpression seems to be localized to the dystrophic myocardium. We suspect that this overexpression indicates the presence of inflammatory cell infiltration—presumably primarily activated macrophages—to the hearts of 8-10-week old dystrophic mice. Although we acknowledge that TSPO is known to be constitutively expressed within cardiac tissue, the mRNA profile of TSPO typically remains at a steady moderate state within normal healthy tissue [42,43]. Importantly, TSPO is found to be overexpressed in inflammatory cardiac foci, seemingly being upregulated in activated immune cells [44,45]. TSPO-PET has similarly been used as a marker of cardiac macrophage infiltration in previous studies of myocarditis, and myocardial infarction [24,44]. As such, it is suggested that these heightened [¹⁸F]FEPPA activities may indicate activated macrophage presence within the murine dystrophic heart.

Macrophage recruitment to the DMD heart is not unique to this study, as the well-known narrative of dystrophic cardiac degeneration is centered around inflammation-exacerbated damage, following dystrophin-deficient cardiac muscle contraction. It is currently hypothesized that similar to the skeletal muscle, these high incidences of inflammation in DMD cardiac tissue may be the result of a longstanding contraction-induced damage cycle caused by dystrophin loss [4,13,46]. The lack of dystrophin protein within cardiomyocytes, shows increased susceptibility of the sarcolemma to damage from muscle contractions, resulting in a “leaky” plasma membrane [13,47]. In addition, dystrophin-deficient cardiomyocytes are found to have significantly impaired L-type calcium channels and mechanical stretch-activated receptors, which normally promote the influx of calcium ions from the extracellular matrix and contribute to depolarization. Due to impaired calcium channels, excessive calcium overflow occurs within cardiomyocytes, which increases reactive oxygen species and subsequently triggers the NF-κB signaling pathway [13,48]. This prompts the further release of inflammatory cytokines and the recruitment of macrophages, lymphocytes, and other cells [49]. This is one possible contributor of cardiac inflammation. Additionally, the improper channel functionality may result in the influx of excess calcium ions, activating proteases within the cell and initiating an auto-digestion process of the remaining myocytes, thus

beginning the cardiac degenerative process [13,47,48]. To help with phagocytosis, these necrotic cardiomyocytes may trigger the recruitment of macrophages, which can release pro-inflammatory cytokines. These cytokines may trigger fibroblasts in the extracellular matrix to produce collagen, leading to fibrosis—particularly in regions of high contractility and movement (e.g. left ventricle) [5,14,15]. As a result, elastic cardiac muscle is replaced with rigid fibrotic tissue, subsequently leading to the iconic cardiomyopathy associated with DMD.

Our data, highlighting the presence of TSPO-bound ligands in DMD subjects and the histological evidence of M1-like (proinflammatory) and M2-like (reparative) macrophage infiltration into the sites of DMD injury support this hypothesis [50–52]. Interestingly, these suspected elevations in inflammatory load are observed quite early at 8-10 weeks—when the *mdx:utrn*(+/-) model heart function is relatively stable. This agrees with earlier reports that indicate a certain degree of inflammation, cellular necrosis, and fibrosis within their myocardium at 10 weeks of age [53]. However, it should be noted that one cardiac DMD murine study found a lack of macrophage infiltration into cardiac tissue until 6 months of age—in contrast to our results [54]. This delayed inflammatory onset might be due to the authors' use of *mdx* mice, a comparatively less severe model than ours, as it is known to demonstrate minimal—if any—cardiac dysfunction [55,56]. Within studies pertaining the same murine model as ours, evidence of ventricular dysfunction (i.e. impaired stroke volume, decreased ejection fraction, and elevated heart rate) were observed far later at 10 months of age, compared to our observed onset of cardiac inflammation at 8-10 weeks [57]. Thus, the present findings may indicate an early onset of cardiac inflammation prior to the onset of cardiac symptoms. Considering that *mdx:utrn*(+/-) mice who were started on an anti-inflammatory quercetin-enriched diet at 8 weeks of age have comparatively minimal cardiac damage than those without, the early detection and intervention to modulate cardiac inflammation may be vital in possibly attenuating downstream DMD cardiac degenerative symptoms [58]. A more extensive explanation of this mechanism is outside of the scope of this paper. However, a further longitudinal study pairing this [¹⁸F]FEPPA PET protocol with an anatomical or morphological modality (such as MRI), may be undertaken to better assess how this early

inflammatory response may contribute to the pathology of dystrophic cardiac tissue damage.

[¹⁸F]FEPPA was originally designed and is still commonly used to assess activated microglia, as an analogue of neuroinflammation. *In-vivo* [¹⁸F]FEPPA SUV has been correlated with post-mortem pro-inflammatory markers histologically in other neuroinflammatory or disease models, validating its use as an analogue of activated microglia cells [59]. In the current study, *in-vivo* [¹⁸F]FEPPA signal within the whole brain was found to correlate with *ex-vivo* TSPO immunofluorescence intensity, suggesting the possible localization of activated microglia to the dystrophic neural tissue. To the best of our knowledge, there are no other study demonstrating the presence of immune cell infiltration into the dystrophic brain. However in support of our observations, heightened levels of pro-inflammatory cytokines interleukin (IL)-1 β and Tumor Necrosis Factor (TNF)- α (molecules commonly associated with neurological immune response) have been found within the brains of *mdx* mice, who also displayed cognitive impairment similar to those in DMD patients [22]. Recent literature has also speculated that these specific cytokines may participate in the emergence of DMD cognitive dysfunction symptoms by altering several features in synaptic transmission (see review in Rae and O'Malley [60] and Stephenson et al. [61]). Considering that activated microglia are known to upregulate TSPO expression and release pro-inflammatory cytokines (e.g. IL-1 β , IL-6, TNF- α), it is possible that the activated microglia may contribute to the dystrophic brain's impairment [24,62,63]. Additionally, the activated microglia may also predict cognitive deterioration as multiple studies regarding neurodegenerative diseases—such as Alzheimer's dementia—have reported that the degree of neuroinflammation can predict longitudinal cognitive decline [64]. Similarly, it is widely accepted that the earliest manifestation of some neurodegenerative diseases is microgliosis, which are evident before the onset of clinical symptoms [65,66]. While the underlying mechanism on how activated microglia contributes to downstream neurodegeneration is still under debate, the early observation of neuroinflammation within our study and the knowledge of late-onset cognitive decline within both older DMD patients (occurring at 30 years of age) and aged murine models (occurring at 18 months) suggests a possible similar association [10,12]. As such, a future study using

TSPO-PET to longitudinally assess neuroinflammation in these DMD murine models—alongside cognitive testing—is suggested to better delineate the relationship between early neuroinflammation and late-onset cognitive decline.

A possible explanation for this microglia activation within the brain may, in part, be due to pro-inflammatory cytokines—which are abundant in DMD circulation—passing through the “leaky” dystrophin-deficient blood-brain barrier (BBB) [4]. Within the brain, dystrophin—specifically Dp71—is located in the perivascular end-feet of astrocytes, normally participating in the stabilization and regulation of molecules transporting through the BBB [67]. In *mdx* mice, the reduction of Dp71 demonstrates severe alteration of endothelial and glial cells, as well as a reduction in the expression of zonula occludens and Aquaporin-4. As a result, *mdx* mice shows increased vascular permeability and by proxy, increased permeability of the BBB [67–69]. Increased BBB permeability and IL-6 levels within the brain were shown when systemic inflammation was induced by a peripheral lipopolysaccharide injection to an Alzheimer’s APP transgenic mouse, resulting in more severe cognitive symptoms [70]. Thus we speculate that the nature of this [¹⁸F]FEPPA uptake and subsequent TSPO overexpression within the brain may be due a result of a similar incidence. However, it should be noted that within a study investigating the permeability of the BBB in *mdx* mice, CD4-, CD8-, CD20- and CD68-positive cells were not histologically observed within the BBB perivascular stroma [71]. These observations, while contrasting, do not conflict with our findings as alternate passages of cytokines through the BBB has already been extensively investigated [72,73]. A possible source of systemic inflammation/pro-inflammatory cytokines within our study include the dystrophin-deficient cardiac and skeletal muscles—which as stated before are known to sustain critical damage upon sarcolemma contraction and release pro-inflammatory cytokines into circulation. The concomitant TSPO-tracer uptake within both the heart and brain and our autoradiography and biodistribution results (i.e. trends towards heightened binding across almost all tissue types) speaks to the systemic nature of inflammation within DMD, while hinting its possible contribution to both downstream cardiac and neurodegeneration damage. It will be interesting to investigate if the neuroinflammation observed in this DMD mice model is widespread across the whole brain, or specific to certain regions, especially in the hippocampus where atrophy within

this region has been linked to progressive cognitive impairment in DMD mice [12]. Further PET/MRI studies linking [¹⁸F]FEPPA PET to regional MRI volumetry and functional MRI network changes will help shed more light.

The strengths of our study include: 1) the utility of non-invasive inflammation imaging using second generation TSPO radioligand [¹⁸F]FEPPA, 2) the use of a high-resolution (1.4–1.5mm) small animal PET scanner capable of multi-organ/whole-body image data acquisition, and 3) the showcase of tissue-specific dosimetry and molecular colocalization capabilities via biodistribution and autoradiography respectively in a DMD murine models—allowing for the additional *in-vitro* histopathological validation of our *in-vivo* imaging studies. However, this study also has several limitations. Firstly, the study sample size is relatively small and uses a mixed sex murine cohort despite DMD being a X-linked genetic disorder and thus, primarily appearing in only human male patients. While this is a common notion in DMD pre-clinical literature since both sexes can express this phenotype through mutations in their dystrophic and utrophin genes, there have been reports that female patients and rodents express constitutively higher levels of TSPO in both cardiac and neural tissue [56,74–76]. Due to low sample sizes, we could not account for these potential sex differences with this study; however, a fair balance between sexes were used (wild-type: 2 females, 4 males; DMD: 2 females, 2 males). Secondly, similar to other TSPO-PET literature, [¹⁸F]FEPPA is unable to differentiate between macrophage/microglia morphological states (i.e. pro-inflammatory and anti-inflammatory). Lastly, while [¹⁸F]FEPPA is commonly used to assess activated microglia, it is difficult to discern the true sensitivity of this tracer within DMD as TSPO is also present in astrocytes, pericytes, and endothelial cells, among other structures within the brain at low levels. During DMD, astrocytes may be activated due to a lack of functional dystrophin, as its absence can precipitate a series of complex signalling cascades that leads to glutamate toxicity in the CNS [77]. However, it should be noted that the percentage of cells expressing TSPO are reported to be ~7 times higher for microglia than for astrocytes, as measured by scRNA-seq—suggesting a preference for the TSPO radiotracer to bind to microglia [78]. Thus, it is suggested that further multi-tracer studies using both [¹⁸F]FEPPA and specific PET tracers targeting solely activated macrophages or microglia such as triggering receptor expressed on myeloid cells

(TREM) can be used to further validate the use of [^{18}F]FEPPA as a multi-organ inflammation assessment tool in DMD [79].

2.5 Conclusions

This exploratory study demonstrated that dystrophin-deficient subjects were associated with higher inflammatory [^{18}F]FEPPA radiotracer binding, mirroring *ex-vivo* histological TSPO data within both their hearts and their brains, and suggesting the presence of early-onset cardiac- and neuroinflammation. Thus, TSPO-PET might be a useful tool for the *in-vivo* assessment of chronic inflammation in several organs simultaneously, particularly within a dystrophic disease.

2.6 Acknowledgements

We thank Dr. Matthew Fox, Haris Smailovic, and Lise Desjardins who assisted in PET/autoradiography operations. Thanks to the members of the Hoffman lab for performing a portion of the animal care and handling. [116]

2.7 References

- [1] Bushby K, Finkel R, Birnkrant DJ, Case LE, Clemens PR, Cripe L, et al. Diagnosis and management of Duchenne muscular dystrophy, part 1: diagnosis, and pharmacological and psychosocial management. *Lancet Neurol* 2010;9:77–93. [https://doi.org/10.1016/S1474-4422\(09\)70271-6](https://doi.org/10.1016/S1474-4422(09)70271-6).
- [2] Ueda Y. Cognitive Function and Quality of Life of Muscular Dystrophy. *Muscular Dystrophies* 2019. <https://doi.org/10.5772/intechopen.86222>.
- [3] Doorenweerd N. Combining genetics, neuropsychology and neuroimaging to improve understanding of brain involvement in Duchenne muscular dystrophy - a narrative review. *Neuromuscul Disord* 2020;30:437–42. <https://doi.org/10.1016/j.nmd.2020.05.001>.
- [4] Rosenberg AS, Puig M, Nagaraju K, Hoffman EP, Villalta SA, Rao VA, et al. Immune-mediated pathology in Duchenne muscular dystrophy. *Sci Transl Med* 2015;7:299rv4. <https://doi.org/10.1126/scitranslmed.aaa7322>.
- [5] D'Amario D, Amodeo A, Adorisio R, Tiziano FD, Leone AM, Perri G, et al. A current approach to heart failure in Duchenne muscular dystrophy. *Heart* 2017;103:1770–9. <https://doi.org/10.1136/heartjnl-2017-311269>.
- [6] Shin J, Tajrishi MM, Ogura Y, Kumar A. Wasting mechanisms in muscular dystrophy. *Int J Biochem Cell Biol* 2013;45:2266–79. <https://doi.org/10.1016/j.biocel.2013.05.001>.
- [7] Eagle M, Baudouin SV, Chandler C, Giddings DR, Bullock R, Bushby K. Survival in Duchenne muscular dystrophy: improvements in life expectancy since 1967 and the impact of home nocturnal ventilation. *Neuromuscul Disord* 2002;12:926–9. [https://doi.org/10.1016/S0960-8966\(02\)00140-2](https://doi.org/10.1016/S0960-8966(02)00140-2).
- [8] Nigro G, Comi LI, Politano L, Bain RJ. The incidence and evolution of cardiomyopathy in Duchenne muscular dystrophy. *Int J Cardiol* 1990;26:271–7. [https://doi.org/10.1016/0167-5273\(90\)90082-g](https://doi.org/10.1016/0167-5273(90)90082-g).
- [9] Ballard E, Grey N, Jungbluth H, Wraige E, Kapetanakis S, Davidson C, et al. Observation cohort study of cause of death in patients with Duchenne muscular dystrophy (DMD). *Eur Respir J* 2012;40.
- [10] Ueda Y, Suwazono S, Maedo S, Higuchi I. Profile of cognitive function in adults with duchenne muscular dystrophy. *Brain Dev* 2017;39:225–30. <https://doi.org/10.1016/j.braindev.2016.10.005>.
- [11] Cotton S, Voudouris NJ, Greenwood KM. Intelligence and Duchenne muscular dystrophy: Full-Scale, Verbal, and Performance intelligence quotients. *Dev Med*

- Child Neurol 2007;43:497–501. <https://doi.org/10.1111/j.1469-8749.2001.tb00750.x>.
- [12] Bagdatlioglu E, Porcari P, Greally E, Blamire AM, Straub VW. Cognitive impairment appears progressive in the mdx mouse. *Neuromuscul Disord* 2020;30:368–88. <https://doi.org/10.1016/j.nmd.2020.02.018>.
- [13] Johnstone VPA, Viola HM, Hool LC. Dystrophic Cardiomyopathy-Potential Role of Calcium in Pathogenesis, Treatment and Novel Therapies. *Genes* 2017;8. <https://doi.org/10.3390/genes8040108>.
- [14] Nitahara-Kasahara Y, Takeda S, Okada T. Inflammatory predisposition predicts disease phenotypes in muscular dystrophy. *Inflamm Regen* 2016;36:14. <https://doi.org/10.1186/s41232-016-0019-0>.
- [15] Meyers TA, Townsend D. Cardiac Pathophysiology and the Future of Cardiac Therapies in Duchenne Muscular Dystrophy. *Int J Mol Sci* 2019;20. <https://doi.org/10.3390/ijms20174098>.
- [16] Snow WM, Anderson JE, Jakobson LS. Neuropsychological and neurobehavioral functioning in Duchenne muscular dystrophy: a review. *Neurosci Biobehav Rev* 2013;37:743–52. <https://doi.org/10.1016/j.neubiorev.2013.03.016>.
- [17] Winterholler Martin, Holländer Christian, Kerling Frank, Weber Irina, Dittrich Sven, Türk Matthias, et al. Stroke in Duchenne Muscular Dystrophy. *Stroke* 2016;47:2123–6. <https://doi.org/10.1161/STROKEAHA.116.013678>.
- [18] Ahmad N, Welch I, Grange R, Hadway J, Dhanvantari S, Hill D, et al. Use of imaging biomarkers to assess perfusion and glucose metabolism in the skeletal muscle of dystrophic mice. *BMC Musculoskelet Disord* 2011;12:127. <https://doi.org/10.1186/1471-2474-12-127>.
- [19] Lim M. Treating inflammation in childhood neurodegenerative disorders. *Dev Med Child Neurol* 2011;53:298–304. <https://doi.org/10.1111/j.1469-8749.2010.03902.x>.
- [20] Mavrogeni S, Papavasiliou A, Spargias K, Constandoulakis P, Papadopoulos G, Karanasios E, et al. Myocardial inflammation in Duchenne Muscular Dystrophy as a precipitating factor for heart failure: a prospective study. *BMC Neurol* 2010;10:33. <https://doi.org/10.1186/1471-2377-10-33>.
- [21] Chen W-W, Zhang X, Huang W-J. Role of neuroinflammation in neurodegenerative diseases (Review). *Mol Med Rep* 2016;13:3391–6. <https://doi.org/10.3892/mmr.2016.4948>.
- [22] Comim CM, Ventura L, Freiberger V, Dias P, Bragagnolo D, Dutra ML, et al. Neurocognitive Impairment in mdx Mice. *Mol Neurobiol* 2019;56:7608–16. <https://doi.org/10.1007/s12035-019-1573-7>.

- [23] Aarli J. Role of Cytokines in Neurological Disorders. *Curr Med Chem* 2003;10:1931–7. <https://doi.org/10.2174/0929867033456918>.
- [24] Thackeray JT, Hupe HC, Wang Y, Bankstahl JP, Berding G, Ross TL, et al. Myocardial Inflammation Predicts Remodeling and Neuroinflammation After Myocardial Infarction. *J Am Coll Cardiol* 2018;71:263–75. <https://doi.org/10.1016/j.jacc.2017.11.024>.
- [25] Wilson AA, Garcia A, Parkes J, McCormick P, Stephenson KA, Houle S, et al. Radiosynthesis and initial evaluation of [18F]-FEPPA for PET imaging of peripheral benzodiazepine receptors. *Nucl Med Biol* 2008;35:305–14. <https://doi.org/10.1016/j.nucmedbio.2007.12.009>.
- [26] Grady RM, Teng H, Nichol MC, Cunningham JC, Wilkinson RS, Sanes JR. Skeletal and Cardiac Myopathies in Mice Lacking Utrophin and Dystrophin: A Model for Duchenne Muscular Dystrophy. *Cell* 1997;90:729–38. [https://doi.org/10.1016/S0092-8674\(00\)80533-4](https://doi.org/10.1016/S0092-8674(00)80533-4).
- [27] Homma S, Kaul S, Boucher CA. Correlates of lung/heart ratio of thallium-201 in coronary artery disease. *J Nucl Med Off Publ Soc Nucl Med* 1987;28:1531–5.
- [28] Gage GJ, Kipke DR, Shain W. Whole Animal Perfusion Fixation for Rodents. *JoVE J Vis Exp* 2012:e3564. <https://doi.org/10.3791/3564>.
- [29] Schindelin J, Arganda-Carreras I, Frise E, Kaynig V, Longair M, Pietzsch T, et al. Fiji: an open-source platform for biological-image analysis. *Nat Methods* 2012;9:676–82. <https://doi.org/10.1038/nmeth.2019>.
- [30] Cuhlmann S, Gsell W, Van der Heiden K, Habib J, Tremoleda JL, Khalil M, et al. In vivo mapping of vascular inflammation using the translocator protein tracer 18F-FEDAA1106. *Mol Imaging* 2014;13. <https://doi.org/10.2310/7290.2014.00014>.
- [31] Largeau B, Dupont A-C, Guilloteau D, Santiago-Ribeiro M-J, Arlicot N. TSPO PET Imaging: From Microglial Activation to Peripheral Sterile Inflammatory Diseases? *Contrast Media Mol Imaging* 2017;2017:1–17. <https://doi.org/10.1155/2017/6592139>.
- [32] Gerhard A, Neumaier B, Elitok E, Glatting G, Ries V, Tomczak R, et al. In vivo imaging of activated microglia using [11C]PK11195 and positron emission tomography in patients after ischemic stroke. *Neuroreport* 2000;11:2957–60. <https://doi.org/10.1097/00001756-200009110-00025>.
- [33] Schneider SM, Sridhar V, Bettis AK, Heath-Barnett H, Balog-Alvarez CJ, Guo L-J, et al. Glucose Metabolism as a Pre-clinical Biomarker for the Golden Retriever Model of Duchenne Muscular Dystrophy. *Mol Imaging Biol* 2018;20:780–8. <https://doi.org/10.1007/s11307-018-1174-2>.

- [34] Lee JS, Pfund Z, Juhász C, Behen ME, Muzik O, Chugani DC, et al. Altered regional brain glucose metabolism in Duchenne muscular dystrophy: A pet study: FDG PET in Duchenne Dystrophy. *Muscle Nerve* 2002;26:506–12. <https://doi.org/10.1002/mus.10238>.
- [35] Bresolin N, Castelli E, Comi GP, Felisari G, Bardoni A, Perani D, et al. Cognitive impairment in Duchenne muscular dystrophy. *Neuromuscul Disord NMD* 1994;4:359–69. [https://doi.org/10.1016/0960-8966\(94\)90072-8](https://doi.org/10.1016/0960-8966(94)90072-8).
- [36] Basu S, Zhuang H, Torigian DA, Rosenbaum J, Chen W, Alavi A. Functional imaging of inflammatory diseases using nuclear medicine techniques. *Semin Nucl Med* 2009;39:124–45. <https://doi.org/10.1053/j.semnuclmed.2008.10.006>.
- [37] Jeong YJ, Yoon HJ, Kang D-Y. Assessment of change in glucose metabolism in white matter of amyloid-positive patients with Alzheimer disease using F-18 FDG PET. *Medicine (Baltimore)* 2017;96. <https://doi.org/10.1097/MD.00000000000009042>.
- [38] MacRitchie N, Frleta-Gilchrist M, Sugiyama A, Lawton T, McInnes IB, Maffia P. Molecular imaging of inflammation - Current and emerging technologies for diagnosis and treatment. *Pharmacol Ther* 2020;211:107550. <https://doi.org/10.1016/j.pharmthera.2020.107550>.
- [39] Lange PS, Avramovic N, Frommeyer G, Wasmer K, Pott C, Eckardt L, et al. Routine 18F-FDG PET/CT does not detect inflammation in the left atrium in patients with atrial fibrillation. *Int J Cardiovasc Imaging* 2017;33:1271–6. <https://doi.org/10.1007/s10554-017-1094-2>.
- [40] Brendel M, Probst F, Jaworska A, Overhoff F, Korzhova V, Albert NL, et al. Glial Activation and Glucose Metabolism in a Transgenic Amyloid Mouse Model: A Triple-Tracer PET Study. *J Nucl Med Off Publ Soc Nucl Med* 2016;57:954–60. <https://doi.org/10.2967/jnumed.115.167858>.
- [41] Zimmer ER, Parent MJ, Souza DG, Leuzy A, Lecrux C, Kim H-I, et al. [18F]FDG PET signal is driven by astroglial glutamate transport. *Nat Neurosci* 2017;20:393–5. <https://doi.org/10.1038/nn.4492>.
- [42] Giatzakis C, Papadopoulos V. Differential utilization of the promoter of peripheral-type benzodiazepine receptor by steroidogenic versus nonsteroidogenic cell lines and the role of Sp1 and Sp3 in the regulation of basal activity. *Endocrinology* 2004;145:1113–23. <https://doi.org/10.1210/en.2003-1330>.
- [43] Gavish M, Bachman I, Shoukrun R, Katz Y, Veenman L, Weisinger G, et al. Enigma of the peripheral benzodiazepine receptor. *Pharmacol Rev* 1999;51:629–50.
- [44] Kim GR, Paeng JC, Jung JH, Moon BS, Lopalco A, Denora N, et al. Assessment of TSPO in a Rat Experimental Autoimmune Myocarditis Model: A Comparison

- Study between [18F]Fluoromethyl-PBR28 and [18F]CB251. *Int J Mol Sci* 2018;19. <https://doi.org/10.3390/ijms19010276>.
- [45] Qi X, Xu J, Wang F, Xiao J. Translocator Protein (18 kDa): A Promising Therapeutic Target and Diagnostic Tool for Cardiovascular Diseases. *Oxid Med Cell Longev* 2012;2012:e162934. <https://doi.org/10.1155/2012/162934>.
- [46] Li Y, Ge S, Peng Y, Chen X. Inflammation and cardiac dysfunction during sepsis, muscular dystrophy, and myocarditis. *Burns Trauma* 2013;1:109–21. <https://doi.org/10.4103/2321-3868.123072>.
- [47] Shirokova N, Niggli E. Cardiac Phenotype of Duchenne Muscular Dystrophy: Insights from Cellular Studies. *J Mol Cell Cardiol* 2013;58:217–24. <https://doi.org/10.1016/j.yjmcc.2012.12.009>.
- [48] Deconinck N, Dan B. Pathophysiology of duchenne muscular dystrophy: current hypotheses. *Pediatr Neurol* 2007;36:1–7. <https://doi.org/10.1016/j.pediatrneurol.2006.09.016>.
- [49] Henríquez-Olguín C, Altamirano F, Valladares D, López JR, Allen PD, Jaimovich E. Altered ROS production, NF- κ B activation and interleukin-6 gene expression induced by electrical stimulation in dystrophic mdx skeletal muscle cells. *Biochim Biophys Acta BBA - Mol Basis Dis* 2015;1852:1410–9. <https://doi.org/10.1016/j.bbadis.2015.03.012>.
- [50] Villalta SA, Nguyen HX, Deng B, Gotoh T, Tidball JG. Shifts in macrophage phenotypes and macrophage competition for arginine metabolism affect the severity of muscle pathology in muscular dystrophy. *Hum Mol Genet* 2009;18:482–96. <https://doi.org/10.1093/hmg/ddn376>.
- [51] Bridges LR. The association of cardiac muscle necrosis and inflammation with the degenerative and persistent myopathy of MDX mice. *J Neurol Sci* 1986;72:147–57. [https://doi.org/10.1016/0022-510x\(86\)90003-1](https://doi.org/10.1016/0022-510x(86)90003-1).
- [52] Nitahara-Kasahara Y, Hayashita-Kinoh H, Chiyo T, Nishiyama A, Okada H, Takeda S, et al. Dystrophic mdx mice develop severe cardiac and respiratory dysfunction following genetic ablation of the anti-inflammatory cytokine IL-10. *Hum Mol Genet* 2014;23:3990–4000. <https://doi.org/10.1093/hmg/ddu113>.
- [53] Hainsey TA, Senapati S, Kuhn DE, Rafael JA. Cardiomyopathic features associated with muscular dystrophy are independent of dystrophin absence in cardiovascular. *Neuromuscul Disord NMD* 2003;13:294–302. [https://doi.org/10.1016/s0960-8966\(02\)00286-9](https://doi.org/10.1016/s0960-8966(02)00286-9).
- [54] Van Erp C, Loch D, Laws N, Trebbin A, Hoey AJ. Timeline of cardiac dystrophy in 3-18-month-old MDX mice. *Muscle Nerve* 2010;42:504–13. <https://doi.org/10.1002/mus.21716>.

- [55] Yucel N, Chang AC, Day JW, Rosenthal N, Blau HM. Humanizing the mdx mouse model of DMD: the long and the short of it. *NPJ Regen Med* 2018;3:4. <https://doi.org/10.1038/s41536-018-0045-4>.
- [56] Gutpell KM, Hrinivich WT, Hoffman LM. Skeletal Muscle Fibrosis in the mdx/utrn+/- Mouse Validates Its Suitability as a Murine Model of Duchenne Muscular Dystrophy. *PLoS ONE* 2015;10. <https://doi.org/10.1371/journal.pone.0117306>.
- [57] Verhaart IEC, Duijn RJM van, Adel B den, Roest AAW, Verschuuren JJGM, Aartsma-Rus A, et al. Assessment of cardiac function in three mouse dystrophinopathies by magnetic resonance imaging. *Neuromuscul Disord* 2012;22:418–26. <https://doi.org/10.1016/j.nmd.2011.10.025>.
- [58] Ballmann C, Denney TS, Beyers RJ, Quindry T, Romero M, Amin R, et al. Lifelong quercetin enrichment and cardioprotection in Mdx/Utrn+/- mice. *Am J Physiol-Heart Circ Physiol* 2016;312:H128–40. <https://doi.org/10.1152/ajpheart.00552.2016>.
- [59] Zammit M, Tao Y, Olsen ME, Metzger J, Vermilyea SC, Bjornson K, et al. [18F]FEPPA PET imaging for monitoring CD68-positive microglia/macrophage neuroinflammation in nonhuman primates. *EJNMMI Res* 2020;10:93. <https://doi.org/10.1186/s13550-020-00683-5>.
- [60] Rae MG, O'Malley D. Cognitive dysfunction in Duchenne muscular dystrophy: a possible role for neuromodulatory immune molecules. *J Neurophysiol* 2016;116:1304–15. <https://doi.org/10.1152/jn.00248.2016>.
- [61] Stephenson KA, Rae MG, O'Malley D. Interleukin-6: A neuro-active cytokine contributing to cognitive impairment in Duchenne muscular dystrophy? *Cytokine* 2020;133:155134. <https://doi.org/10.1016/j.cyto.2020.155134>.
- [62] Sawada M, Kondo N, Suzumura A, Marunouchi T. Production of tumor necrosis factor-alpha by microglia and astrocytes in culture. *Brain Res* 1989;491:394–7. [https://doi.org/10.1016/0006-8993\(89\)90078-4](https://doi.org/10.1016/0006-8993(89)90078-4).
- [63] Hanisch U-K. Microglia as a source and target of cytokines. *Glia* 2002;40:140–55. <https://doi.org/10.1002/glia.10161>.
- [64] Malpetti M, Kievit RA, Passamonti L, Jones PS, Tsvetanov KA, Rittman T, et al. Microglial activation and tau burden predict cognitive decline in Alzheimer's disease. *Brain* 2020;143:1588–602. <https://doi.org/10.1093/brain/awaa088>.
- [65] Yoshiyama Y, Higuchi M, Zhang B, Huang S-M, Iwata N, Saido TC, et al. Synapse loss and microglial activation precede tangles in a P301S tauopathy mouse model. *Neuron* 2007;53:337–51. <https://doi.org/10.1016/j.neuron.2007.01.010>.

- [66] Ponomarev ED, Shriver LP, Maresz K, Dittel BN. Microglial cell activation and proliferation precedes the onset of CNS autoimmunity. *J Neurosci Res* 2005;81:374–89. <https://doi.org/10.1002/jnr.20488>.
- [67] Naidoo M, Anthony K. Dystrophin Dp71 and the Neuropathophysiology of Duchenne Muscular Dystrophy. *Mol Neurobiol* 2020;57:1748–67. <https://doi.org/10.1007/s12035-019-01845-w>.
- [68] Nico B, Tamma R, Annese T, Mangieri D, De Luca A, Corsi P, et al. Glial dystrophin-associated proteins, laminin and agrin, are downregulated in the brain of mdx mouse. *Lab Investig J Tech Methods Pathol* 2010;90:1645–60. <https://doi.org/10.1038/labinvest.2010.149>.
- [69] Nico B, Paola Nicchia G, Frigeri A, Corsi P, Mangieri D, Ribatti D, et al. Altered blood–brain barrier development in dystrophic MDX mice. *Neuroscience* 2004;125:921–35. <https://doi.org/10.1016/j.neuroscience.2004.02.008>.
- [70] Takeda S, Sato N, Ikimura K, Nishino H, Rakugi H, Morishita R. Increased blood–brain barrier vulnerability to systemic inflammation in an Alzheimer disease mouse model. *Neurobiol Aging* 2013;34:2064–70. <https://doi.org/10.1016/j.neurobiolaging.2013.02.010>.
- [71] Nico B, Frigeri A, Nicchia GP, Corsi P, Ribatti D, Quondamatteo F, et al. Severe alterations of endothelial and glial cells in the blood-brain barrier of dystrophic mdx mice. *Glia* 2003;42:235–51. <https://doi.org/10.1002/glia.10216>.
- [72] Gutierrez EG, Banks WA, Kastin AJ. Murine tumor necrosis factor alpha is transported from blood to brain in the mouse. *J Neuroimmunol* 1993;47:169–76. [https://doi.org/10.1016/0165-5728\(93\)90027-v](https://doi.org/10.1016/0165-5728(93)90027-v).
- [73] Banks WA, Kastin AJ, Broadwell RD. Passage of cytokines across the blood-brain barrier. *Neuroimmunomodulation* 1995;2:241–8. <https://doi.org/10.1159/000097202>.
- [74] Gutpell KM, Tasevski N, Wong B, Hrinivich WT, Su F, Hadway J, et al. ANG1 treatment reduces muscle pathology and prevents a decline in perfusion in DMD mice. *PLOS ONE* 2017;12:e0174315. <https://doi.org/10.1371/journal.pone.0174315>.
- [75] Fairweather D, Coronado MJ, Garton AE, Dziedzic JL, Bucek A, Cooper LT, et al. Sex differences in translocator protein 18 kDa (TSPO) in the heart: implications for imaging myocardial inflammation. *J Cardiovasc Transl Res* 2014;7:192–202. <https://doi.org/10.1007/s12265-013-9538-0>.
- [76] Tuisku J, Plavén-Sigraý P, Gaiser EC, Airas L, Al-Abdulrasul H, Brück A, et al. Effects of age, BMI and sex on the glial cell marker TSPO — a multicentre [11C]PBR28 HRRT PET study. *Eur J Nucl Med Mol Imaging* 2019;46:2329–38. <https://doi.org/10.1007/s00259-019-04403-7>.

- [77] Patel AM, Wierda K, Thorrez L, van Putten M, De Smedt J, Ribeiro L, et al. Dystrophin deficiency leads to dysfunctional glutamate clearance in iPSC derived astrocytes. *Transl Psychiatry* 2019;9:200. <https://doi.org/10.1038/s41398-019-0535-1>.
- [78] Notter T, Schalbetter SM, Clifton NE, Mattei D, Richetto J, Thomas K, et al. Neuronal activity increases translocator protein (TSPO) levels. *Mol Psychiatry* 2020:1–13. <https://doi.org/10.1038/s41380-020-0745-1>.
- [79] Liu Q, Johnson EM, Lam RK, Wang Q, Bo Ye H, Wilson EN, et al. Peripheral TREM1 responses to brain and intestinal immunogens amplify stroke severity. *Nat Immunol* 2019;20:1023–34. <https://doi.org/10.1038/s41590-019-0421-2>.

Chapter 3

3 Conclusions and Future Directions

3.1 Study Summary

The aim of this thesis was to primarily explore the use of [^{18}F]FEPPA PET for non-invasive imaging of *in-vivo* inflammatory involvement in the heart and brain of *mdx:utr**n*(+/-) mice. From this thesis, two main conclusions were reached: 1) the dystrophic heart and brain are associated with significant inflammation, and 2) [^{18}F]FEPPA PET is able to assess multi-organ inflammatory load within murine models of DMD.

We demonstrated that 8-10 week old *mdx:utr**n*(+/-) mice had higher [^{18}F]FEPPA uptake in their heart and brains compared to age-matched healthy counterparts, which correlated with heightened *ex-vivo* TSPO levels in our histological data. Preliminary autoradiography and biodistribution also demonstrated the potential *ex-vivo* use of [^{18}F]FEPPA to assess inflammatory load within other organs—indicating the feasibility of this imaging tool as a useful multi-organ assessment tool for inflammation as a result of DMD.

The heightened [^{18}F]FEPPA uptake in the dystrophic heart may be a result of activated cardiac macrophage recruitment to regions of contraction-induced damage caused by dystrophin-loss [1]. However, we speculate that since its onset is observed far earlier than cardiac dysfunction (typically observed at 10 months of age in murine models), this early inflammatory response may contribute to the downstream pathology of dystrophic cardiac tissue damage. Similar incidences of heightened TSPO expression was also observed within the dystrophic brain, which may be the result of microglial cells activation. BBB disruption by a lack of dystrophin may be one of the driving causes, as its increased permeability leads to pro-inflammatory cytokine infiltration [2–4]. As activated microglia may act as both a source and target of inflammatory cytokines, it is

possible that the cytokine-mediated cognitive impairment hypothesis within the dystrophic brain can be mediated by activated microglia [3–6].

3.2 Significance

With increased DMD patient longevity, there have been growing concerns in identifying and treating later onset of symptoms in other organs—specifically within the heart and brain—associated with the later stages of DMD [7–9]. As inflammation is reputedly widespread within both dystrophic skeletal and cardiac muscle, and is becoming a growing concern within the dystrophic brain, the subsequent development of anti-inflammatory therapies that could be implemented prior to onset of severe cardiac or neurological damage can be considered [1,3,10]. As such, the main significance of this research lies in its contribution to the better understanding of inflammation—specifically through providing a tool for researchers to better assess inflammatory load within multiple dystrophic organs at once. The use of [¹⁸F]FEPPA imaging is novel, as this work is the first to utilise a specific inflammatory PET tracer (TSPO) within *mdx* mice rather than using the more conventional [¹⁸F]FDG (which have only been assessed in terms of glucose consumption previously) [11–13]. Additionally, the use of PET in conjunction with autoradiography and biodistribution within our study protocol is also significant. It allows for assessment of inflammation on both an *in-vivo* (via non-invasive PET) and *ex-vivo* (via autoradiography and distribution) level within one specimen, while accounting for potential inter-individual heterogeneity between subjects.

Using [¹⁸F]FEPPA, inflammation is seemingly observable in dystrophic cardiac tissue at 8-10 weeks of age, while signs of neuroinflammation were also present. The observations of neuroinflammation as well as the concurrent presence of cardiac inflammation within the dystrophic subject are novel, as they are the first to demonstrate significant TSPO-upregulation within the dystrophic heart and brain—to which we attribute to activated macrophages and microglia. From these data, the potential avenue of modulating inflammation as a potential therapy is further emphasized.

3.3 Limitations

Our findings within this thesis have profound impact in the field of DMD imaging research. However, as with all studies, there exists some limitations. Firstly, although we discussed our findings with a pro-inflammatory inclination, the inability of [^{18}F]FEPPA to differentiate between pro-inflammatory M1-like and anti-inflammatory M2-like macrophages/microglial cells should be noted [14]. This has been an on-going concern for multiple inflammatory PET analogues—including all the TSPO-PET tracer series as well as the clinically used [^{18}F]FDG. However, amongst a comparative study assessing the inflammatory cell uptake of five candidate inflammation tracers in myocardium, [^{18}F]GE180—another TSPO-targeting PET tracer—showed preferential accumulations in pro-inflammatory M1 macrophages that was seven-fold higher than in M2 [15]. In addition, [^{18}F]GE180 also showed highly selective binding to CD11b+ monocytes over other cell types (i.e. T-cells, natural killer cells), further demonstrating the specificity of TSPO-targeting radiotracers. Considering that [^{18}F]GE180 has 20 times lowered brain penetration than other TSPO tracers—including [^{18}F]PBR28, which is very similar to [^{18}F]FEPPA—we can anticipate better specificity [16]. In addition, it should be noted that *in-vivo* macrophages are not merely classified into M1 or M2 subclasses, but rather will shift its phenotype on a spectrum towards a certain morphology depending on the signals they receive. As such, it is quite possible for macrophages to display a mixed phenotype, having both M1 and M2 characteristics [17,18]. Nonetheless, as the true aim of this was to assess the ability of TSPO-PET to track multi-organ inflammatory load—in which it does—this discrepancy does not take away from this conclusion.

Secondly, while we have used [^{18}F]FEPPA within this study as an analog of activated microglia within the brain, TSPO expression is known to come from several different sources. For instance, TSPO is also constitutively expressed at low levels on astrocytes, pericytes, endothelial cells, among other structures within the brain. These low-levels of expression are not anticipated to cause a discrepancy to our drawn conclusions, as TSPO is typically overexpressed at significantly higher levels under disease conditions. However, it should be noted that reactive astrocytes are also known to overexpress TSPO under certain conditions [19]. This is of concern within our DMD models, as the lack of

dystrophin can trigger a signaling cascade that results in the inhibition of effective glutamate clearance. As glutamate toxicity within the body can prompt astrocyte activation, it is possible that the overexpressed TSPO levels (and subsequent [^{18}F]FEPPA uptake) within the dystrophic brain may not strictly reflect activated microglia [20,21]. However, within a study using scRNA-seq to assess TSPO expression within various neuronal cell populations, the percentage of cells expressing TSPO were reported to be ~7 times higher for microglia than for astrocytes [22]. Thus, while TSPO expression seems to skew towards microglia—thereby supporting our study conclusions—the specificity of TSPO-radiotracer in targeting microglia should be considered in future studies. This is similarly an issue within the heart, as TSPO is also overexpressed by injured cardiomyocytes. Although its involvement is still unclear, the RNA knockout of TSPO in cardiomyocytes post-anoxia/reoxygenation treatment (an analogue of ischemic/reperfusion injury) resulted in inhibited mitochondrial ROS generation and decreased apoptotic cell death [23]. Initially in this thesis, there was the intention of validating the specificity of TSPO through histological co-staining with CD68 or MHCII—which are commonly expressed on activated macrophages and microglia cells [24,25]. Unfortunately, this was not accomplished due to restraints imposed by current global events, but future work in this capacity is suggested to validate the specific contribution of glial cells to DMD cardiac and neurologic outcomes.

Lastly within this thesis, both male and female murine models were used. Despite DMD being more prominently featured in males since it is an X-linked recessive genetic disorder, both sexes exhibit DMD pathogenesis due to mutations in dystrophin and utrophin genes. This is commonplace within DMD literature, as several studies (including our own) use a mixed sex cohort during experimentation [26–28]. However, within an acute myocarditis study, females were reported to constitutively express higher levels of TSPO within cardiac tissue than males prior to disease onset [29]. Similarly, healthy female patients were found to have higher [^{11}C]PBR28 binding across global grey matter, frontal, temporal, occipital and parietal cortices, hippocampus, and thalamus than their males counterparts [30]. Due to low sample sizes, we could not account for sex as a covariate within our statistical analyses; however, a fair balance between sexes were used (wild-type: 2 females, 4 males; DMD: 2 females, 2 males). Nonetheless, future

investigation towards determining the baseline TSPO levels within cardiac and neural tissue of dystrophic subjects is advised.

3.4 Future Directions

The work of this thesis has demonstrated the feasibility of [^{18}F]FEPPA PET as a non-invasive tool to assess multi-organ inflammatory involvement *in-vivo* and investigated the presence of inflammatory load within the dystrophic heart and brain of *mdx:utrn*(+/-) mice. While the conclusions drawn are useful to the field of inflammatory imaging as well as to DMD research in general, there are still additional questions to be answered.

We demonstrated the presence of immune cells within the dystrophic heart and brain histologically and with PET imaging. A future area of interest is in the pairing of our imaging protocol with an additional modality (e.g. MRI or CT) to discern the presence of any anatomical or functional outcomes associated with or co-localized to inflammatory involvement. Histologically, in the DMD heart, inflammatory foci concentrate to regions of cardiac damage (i.e. tissue necrosis, fibrosis, lesions) [31]. While, some DMD boys have indicated signs of brain atrophy in some computed tomography (CT) and MRI scans [32,33]. As such, these future studies may be useful in delineating the contribution of activated macrophages and microglia to dystrophic cardiac and neurological morphological outcomes.

As one of the major benefits of our imaging protocol is its *in-vivo* and minimally invasive nature, another future direction is the longitudinal imaging of inflammation throughout disease progression. Within this exploratory study, we have demonstrated the possible presence of inflammatory cells in DMD mice at the 8-10 week time point, despite *mdx* mice studies reporting cardiomyopathy symptoms and cognitive degeneration at 10 and 18 months respectively [9,34]. Thus, a study longitudinally imaging *mdx* mice at 4-5 weeks (immature), 8-10 weeks, 15-20 weeks (matured), and ~10 months (aged) should be conducted to gain a better understanding of inflammation throughout age progression. Our [^{18}F]FEPPA PET protocol can also be applied to different *mdx* mouse models—genetically mutated to demonstrate different disease severities—for a greater understanding of disease progression [28,34]. In addition, this protocol may also be

performed in conjunction with echocardiograms or various forms of cognitive tests to assess inflammation in relation to the emergence/evolution of DMD cardiac and neurologic functional outcomes.

Lastly, although our sample size for the biodistribution and autoradiography analyses are admittedly small, its trends (in combination with our PET and histological data) demonstrate the feasibility of an *in-vivo* to *ex-vivo* protocol that can be used to systematically image inflammation. In addition to DMD, there are many other inflammation-associated diseases that yield multi-organ dysfunction such as: multiple sclerosis, rheumatoid arthritis, cardiovascular diseases, etc. [35–37]. Thus, there are several diseases that can utilise this [^{18}F]FEPPA imaging protocol for a more systemic understanding of inflammation within several organs simultaneously on both an *in-vivo* (via non-invasive PET) as well as *ex-vivo* (via autoradiography and biodistribution) level.

3.5 Concluding Remarks

In conclusion, the results of this thesis suggest that [^{18}F]FEPPA PET may be a feasible tool to assess *in-vivo* inflammatory load within multiple dystrophic organs simultaneously. Using this imaging tool, we have demonstrated that dystrophin-deficient mice have heightened levels of activated macrophages and microglia within their hearts and brains respectively—thereby supporting our hypothesis. While it is evident that inflammation is present within the cardiac and neural tissue of DMD subjects, further research is necessary to better understand the contribution of activated immune cells to the dysfunctional outcomes. We anticipate that [^{18}F]FEPPA imaging may be useful in these endeavors.

3.6 References

- [1] Shin J, Tajrishi MM, Ogura Y, Kumar A. Wasting mechanisms in muscular dystrophy. *Int J Biochem Cell Biol* 2013;45:2266–79. <https://doi.org/10.1016/j.biocel.2013.05.001>.
- [2] Nico B, Paola Nicchia G, Frigeri A, Corsi P, Mangieri D, Ribatti D, et al. Altered blood–brain barrier development in dystrophic *mdx* mice. *Neuroscience* 2004;125:921–35. <https://doi.org/10.1016/j.neuroscience.2004.02.008>.
- [3] Rae MG, O’Malley D. Cognitive dysfunction in Duchenne muscular dystrophy: a possible role for neuromodulatory immune molecules. *J Neurophysiol* 2016;116:1304–15. <https://doi.org/10.1152/jn.00248.2016>.
- [4] Stephenson KA, Rae MG, O’Malley D. Interleukin-6: A neuro-active cytokine contributing to cognitive impairment in Duchenne muscular dystrophy? *Cytokine* 2020;133:155134. <https://doi.org/10.1016/j.cyto.2020.155134>.
- [5] Sawada M, Kondo N, Suzumura A, Marunouchi T. Production of tumor necrosis factor-alpha by microglia and astrocytes in culture. *Brain Res* 1989;491:394–7. [https://doi.org/10.1016/0006-8993\(89\)90078-4](https://doi.org/10.1016/0006-8993(89)90078-4).
- [6] Hanisch U-K. Microglia as a source and target of cytokines. *Glia* 2002;40:140–55. <https://doi.org/10.1002/glia.10161>.
- [7] D’Amario D, Amodeo A, Adorisio R, Tiziano FD, Leone AM, Perri G, et al. A current approach to heart failure in Duchenne muscular dystrophy. *Heart* 2017;103:1770–9. <https://doi.org/10.1136/heartjnl-2017-311269>.
- [8] Ueda Y, Suwazono S, Maedo S, Higuchi I. Profile of cognitive function in adults with duchenne muscular dystrophy. *Brain Dev* 2017;39:225–30. <https://doi.org/10.1016/j.braindev.2016.10.005>.
- [9] Bagdatlioglu E, Porcari P, Grealley E, Blamire AM, Straub VW. Cognitive impairment appears progressive in the *mdx* mouse. *Neuromuscul Disord* 2020;30:368–88. <https://doi.org/10.1016/j.nmd.2020.02.018>.
- [10] Rosenberg AS, Puig M, Nagaraju K, Hoffman EP, Villalta SA, Rao VA, et al. Immune-mediated pathology in Duchenne muscular dystrophy. *Sci Transl Med* 2015;7:299rv4. <https://doi.org/10.1126/scitranslmed.aaa7322>.
- [11] Schneider SM, Sridhar V, Bettis AK, Heath-Barnett H, Balog-Alvarez CJ, Guo L-J, et al. Glucose Metabolism as a Pre-clinical Biomarker for the Golden Retriever Model of Duchenne Muscular Dystrophy. *Mol Imaging Biol* 2018;20:780–8. <https://doi.org/10.1007/s11307-018-1174-2>.

- [12] Bresolin N, Castelli E, Comi GP, Felisari G, Bardoni A, Perani D, et al. Cognitive impairment in Duchenne muscular dystrophy. *Neuromuscul Disord NMD* 1994;4:359–69. [https://doi.org/10.1016/0960-8966\(94\)90072-8](https://doi.org/10.1016/0960-8966(94)90072-8).
- [13] Lee JS, Pfund Z, Juhász C, Behen ME, Muzik O, Chugani DC, et al. Altered regional brain glucose metabolism in Duchenne muscular dystrophy: A pet study: FDG PET in Duchenne Dystrophy. *Muscle Nerve* 2002;26:506–12. <https://doi.org/10.1002/mus.10238>.
- [14] Janssen B, Vugts DJ, Windhorst AD, Mach RH. PET Imaging of Microglial Activation—Beyond Targeting TSPO. *Mol J Synth Chem Nat Prod Chem* 2018;23. <https://doi.org/10.3390/molecules23030607>.
- [15] Thackeray J, Ross TL, Bankstahl J, Wester H, Bengel F. Targeting cardiovascular inflammation for imaging: Comparison of the uptake of multiple tracers in leukocyte subpopulations. *J Nucl Med* 2017;58:302–302.
- [16] Zanotti-Fregonara P, Pascual B, Rizzo G, Yu M, Pal N, Beers D, et al. Head-to-head comparison of ¹¹C-PBR28 and 18F-GE180 for the quantification of TSPO in the human brain. *J Nucl Med* 2018;jnumed.117.203109. <https://doi.org/10.2967/jnumed.117.203109>.
- [17] Constanzo J, Midavaine É, Fouquet J, Lepage M, Descoteaux M, Kirby K, et al. Brain irradiation leads to persistent neuroinflammation and long-term neurocognitive dysfunction in a region-specific manner. *Prog Neuropsychopharmacol Biol Psychiatry* 2020;102:109954. <https://doi.org/10.1016/j.pnpbp.2020.109954>.
- [18] Vogel DY, Vereyken EJ, Glim JE, Heijnen PD, Moeton M, van der Valk P, et al. Macrophages in inflammatory multiple sclerosis lesions have an intermediate activation status. *J Neuroinflammation* 2013;10:809. <https://doi.org/10.1186/1742-2094-10-35>.
- [19] Cosenza-Nashat M, Zhao M-L, Suh H-S, Morgan J, Natividad R, Morgello S, et al. Expression of the translocator protein of 18 kDa by microglia, macrophages and astrocytes based on immunohistochemical localization in abnormal human brain. *Neuropathol Appl Neurobiol* 2009;35:306–28. <https://doi.org/10.1111/j.1365-2990.2008.01006.x>.
- [20] Patel AM, Wierda K, Thorrez L, van Putten M, De Smedt J, Ribeiro L, et al. Dystrophin deficiency leads to dysfunctional glutamate clearance in iPSC derived astrocytes. *Transl Psychiatry* 2019;9:200. <https://doi.org/10.1038/s41398-019-0535-1>.
- [21] Pannell M, Economopoulos V, Wilson TC, Kersemans V, Isenegger PG, Larkin JR, et al. Imaging of translocator protein upregulation is selective for pro-inflammatory polarized astrocytes and microglia. *Glia* 2020;68:280–97. <https://doi.org/10.1002/glia.23716>.

- [22] Notter T, Schalbetter SM, Clifton NE, Mattei D, Richetto J, Thomas K, et al. Neuronal activity increases translocator protein (TSPO) levels. *Mol Psychiatry* 2020;1–13. <https://doi.org/10.1038/s41380-020-0745-1>.
- [23] Meng Y, Tian M, Yin S, Lai S, Zhou Y, Chen J, et al. Downregulation of TSPO expression inhibits oxidative stress and maintains mitochondrial homeostasis in cardiomyocytes subjected to anoxia/reoxygenation injury. *Biomed Pharmacother* 2020;121:109588. <https://doi.org/10.1016/j.biopha.2019.109588>.
- [24] Venneti S, Lopresti BJ, Wang G, Bissel SJ, Mathis CA, Meltzer CC, et al. PET imaging of brain macrophages using the peripheral benzodiazepine receptor in a macaque model of neuroAIDS. *J Clin Invest* 2004;113:981–9. <https://doi.org/10.1172/JCI200420227>.
- [25] Hopperton KE, Mohammad D, Trépanier MO, Giuliano V, Bazinet RP. Markers of microglia in post-mortem brain samples from patients with Alzheimer's disease: a systematic review. *Mol Psychiatry* 2018;23:177–98. <https://doi.org/10.1038/mp.2017.246>.
- [26] Huang P, Cheng G, Lu H, Aronica M, Ransohoff RM, Zhou L. Impaired respiratory function in *mdx* and *mdx/utrn*(+/-) mice. *Muscle Nerve* 2011;43:263–7. <https://doi.org/10.1002/mus.21848>.
- [27] Gutpell KM, Tasevski N, Wong B, Hrinivich WT, Su F, Hadway J, et al. ANG1 treatment reduces muscle pathology and prevents a decline in perfusion in DMD mice. *PLOS ONE* 2017;12:e0174315. <https://doi.org/10.1371/journal.pone.0174315>.
- [28] Gutpell KM, Hrinivich WT, Hoffman LM. Skeletal Muscle Fibrosis in the *mdx/utrn*+/- Mouse Validates Its Suitability as a Murine Model of Duchenne Muscular Dystrophy. *PLoS ONE* 2015;10. <https://doi.org/10.1371/journal.pone.0117306>.
- [29] Fairweather D, Coronado MJ, Garton AE, Dziedzic JL, Bucek A, Cooper LT, et al. Sex differences in translocator protein 18 kDa (TSPO) in the heart: implications for imaging myocardial inflammation. *J Cardiovasc Transl Res* 2014;7:192–202. <https://doi.org/10.1007/s12265-013-9538-0>.
- [30] Tuisku J, Plavén-Sigraý P, Gaiser EC, Airas L, Al-Abdulrasul H, Brück A, et al. Effects of age, BMI and sex on the glial cell marker TSPO — a multicentre [¹¹C]PBR28 HRRT PET study. *Eur J Nucl Med Mol Imaging* 2019;46:2329–38. <https://doi.org/10.1007/s00259-019-04403-7>.
- [31] Hainsey TA, Senapati S, Kuhn DE, Rafael JA. Cardiomyopathic features associated with muscular dystrophy are independent of dystrophin absence in cardiovascular. *Neuromuscul Disord* 2003;13:294–302. [https://doi.org/10.1016/s0960-8966\(02\)00286-9](https://doi.org/10.1016/s0960-8966(02)00286-9).

- [32] Doorenweerd N, Straathof CS, Dumas EM, Spitali P, Ginjaar IB, Wokke BH, et al. Reduced cerebral gray matter and altered white matter in boys with Duchenne muscular dystrophy. *Ann Neurol* 2014;76:403–11. <https://doi.org/10.1002/ana.24222>.
- [33] Yoshioka M, Okuno T, Honda Y, Nakano Y. Central nervous system involvement in progressive muscular dystrophy. *Arch Dis Child* 1980;55:589–94. <https://doi.org/10.1136/adc.55.8.589>.
- [34] Yucel N, Chang AC, Day JW, Rosenthal N, Blau HM. Humanizing the mdx mouse model of DMD: the long and the short of it. *NPJ Regen Med* 2018;3:4. <https://doi.org/10.1038/s41536-018-0045-4>.
- [35] Weissert R. The Immune Pathogenesis of Multiple Sclerosis. *J Neuroimmune Pharmacol* 2013;8:857–66. <https://doi.org/10.1007/s11481-013-9467-3>.
- [36] Sattar Naveed, McCarey David W., Capell Hilary, McInnes Iain B. Explaining How “High-Grade” Systemic Inflammation Accelerates Vascular Risk in Rheumatoid Arthritis. *Circulation* 2003;108:2957–63. <https://doi.org/10.1161/01.CIR.0000099844.31524.05>.
- [37] Thackeray JT, Hupe HC, Wang Y, Bankstahl JP, Berding G, Ross TL, et al. Myocardial Inflammation Predicts Remodeling and Neuroinflammation After Myocardial Infarction. *J Am Coll Cardiol* 2018;71:263–75. <https://doi.org/10.1016/j.jacc.2017.11.024>.

Appendices

Appendix A: Approval of Animal Protocols



2017-038:9:

AUP Number: 2017-038
AUP Title: Hoffman Breeding Protocol
Yearly Renewal Date: 05/01/2021

The YEARLY RENEWAL to Animal Use Protocol (AUP) 2017-038 has been approved by the Animal Care Committee (ACC), and will be approved through to the above review date.

Please at this time review your AUP with your research team to ensure full understanding by everyone listed within this AUP.



AUP Number: 2018-140
PI Name: Hoffman, Lisa M
AUP Title: Non-Invasive Imaging of Therapeutics in Mouse Models of DMD
Approval Date: 07/01/2019

Official Notice of Animal Care Committee (ACC) Approval:

Your new Animal Use Protocol (AUP) 2018-140:1: entitled " Non-Invasive Imaging of Therapeutics in Mouse Models of DMD"

has been APPROVED by the Animal Care Committee of the University Council on Animal Care. This approval, although valid for up to four years, is subject to annual Protocol Renewal.

Prior to commencing animal work, please review your AUP with your research team to ensure full understanding by everyone listed within this AUP.

Appendix B: Quantitative autoradiography and Biodistribution of [¹⁸F]FEPPA-injected 8-10 week old *mdx:utrn* (+/-) mice.

The following data were submitted as Supplementary Material in the following manuscript:

Tang JM, McClennan A, Liu L, Hadway J, Ronald J, Hicks JW, Hoffman L, Anazodo UC. *In-vivo* imaging of cardiac and neuroinflammation in Duchenne muscular dystrophy: a [¹⁸F]FEPPA PET study. Submitted to Neuromuscul Disord in August 2020. Under Review. Manuscript ID: NWD-S-20-00539.

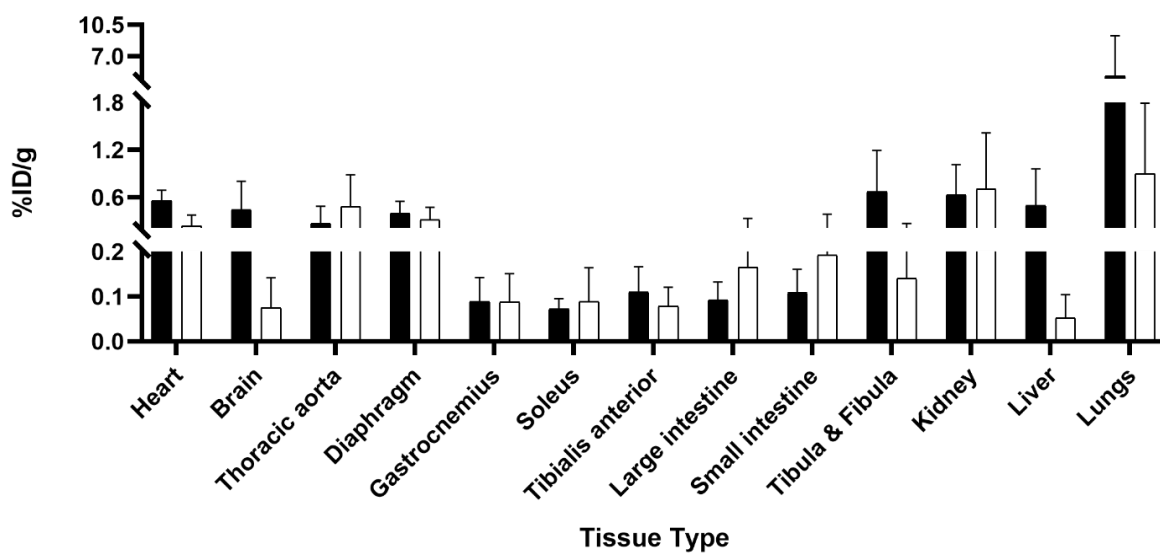


Figure. A.1. Multi-organ Biodistribution of [¹⁸F]FEPPA within murine models. Data (\pm SE) shows the differences in radiotracer uptake as across multiple tissues as the percentage of the injected dose per gram of the tissue (%ID/g) of DMD (black bars; n=4 mice) and age-matched healthy controls (white bars; n=2 mice). No statistical analyses were conducted due to low sample sizes. DMD=Duchenne muscular dystrophy, [¹⁸F]FEPPA=[¹⁸F]-N-(2-(2-fluoroethoxy)benzyl)-N-(4-phenoxy pyridin-3-yl)acetamide.

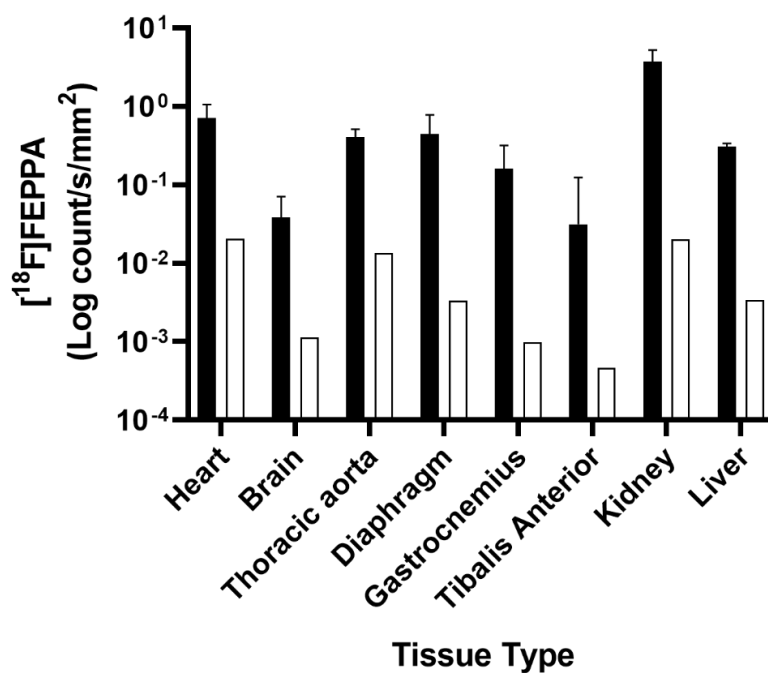


Figure A.2. Quantified autoradiography of [¹⁸F]FEPPA activity in DMD and healthy mice. Data (\pm SE) depicts the log counts per second per millimetre squared area of [¹⁸F]FEPPA activity within slices of heart, brain, thoracic aorta, diaphragm, skeletal muscles, kidney and liver for DMD (black bars; n=3 mice) and an age-matched wild-type control (white bars; n=1 mouse). No statistical analyses were conducted due to low sample sizes. Abbreviations as described in prior figures.

Appendix C: Sample sizes for imaging and histologic studies

The following data were also submitted as Supplementary Material in the following manuscript:

Tang JM, McClennan A, Liu L, Hadway J, Ronald J, Hicks JW, Hoffman L, Anazodo UC. *In-vivo* imaging of cardiac and neuroinflammation in Duchenne muscular dystrophy: a [¹⁸F]FEPPA PET study. Submitted to Neuromuscul Disord in August 2020. Under Review. Manuscript ID: NWD-S-20-00539.

Table A.1. Sample size for the number of unique wild-type and DMD murine subjects were successfully completed for each imaging and histological cohort.

| | PET | Biodistribution | Autoradiography | Immunohistochemistry |
|------------------------------------|-----|-----------------|-----------------|----------------------|
| Wild-type <i>C57Bl10</i> | 6 | 2* | 1 | 3 |
| DMD <i>mdx:utrn(+/-)</i> | 4 | 4* | 3 | 3 |

* indicates the removal of impossible biodistribution values for which measurement errors resulted in negative results (i.e. negative tissue weights stemming from weight of empty tube exceeding the weight of tube&tissue)

Appendix D: Representative qualitative autoradiography images from [¹⁸F]FEPPA-injected 8-10 week old *mdx:utrn (+/-)* mice

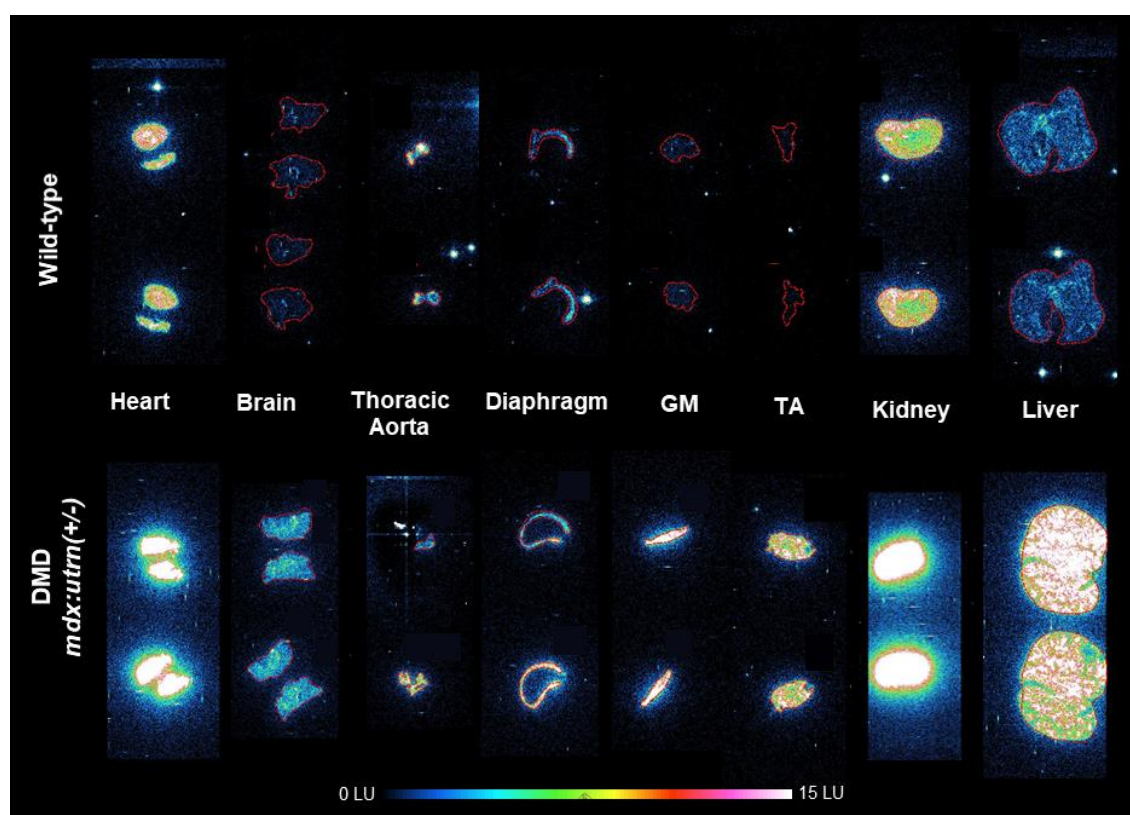


Image depicts autoradiography images of the heart, brain, thoracic aorta, diaphragm, gastrocnemius, tibialis anterior, kidney, and liver tissue excised from [¹⁸F]FEPPA-injected murine models. The representative DMD mouse depicts higher tracer accumulation across all tissue compared to the healthy wild-type control. Regions of tissue are outlined in red. LU=light units.

Appendix E: Copyright Agreement for reproduction of Figure 1.1

8/27/2020

RightsLink Printable License

ELSEVIER LICENSE TERMS AND CONDITIONS

Aug 27, 2020

This Agreement between Ms. Joanne Tang ("You") and Elsevier ("Elsevier") consists of your license details and the terms and conditions provided by Elsevier and Copyright Clearance Center.

| | |
|------------------------------|---|
| License Number | 4897171391249 |
| License date | Aug 27, 2020 |
| Licensed Content Publisher | Elsevier |
| Licensed Content Publication | Journal of the American College of Cardiology |
| Licensed Content Title | Dystrophin-Deficient Cardiomyopathy |
| Licensed Content Author | Forum Kamdar, Daniel J. Garry |
| Licensed Content Date | May 31, 2016 |
| Licensed Content Volume | 67 |
| Licensed Content Issue | 21 |
| Licensed Content Pages | 14 |
| Start Page | 2533 |
| End Page | 2546 |

8/27/2020

RightsLink Printable License

| | |
|--|---|
| Type of Use | reuse in a thesis/dissertation |
| Portion | figures/tables/illustrations |
| Number of figures/tables/illustrations | 1 |
| Format | electronic |
| Are you the author of this Elsevier article? | No |
| Will you be translating? | No |
| Title | An approach for In-vivo characterization of brain and heart inflammation in Duchenne Muscular Dystrophy |
| Institution name | Western University |
| Expected presentation date | Sep 2020 |
| Portions | Figure 2. Schematic Diagram of the DGC |
| Requestor Location | Ms. Joanne Tang [REDACTED] Attn: Western University |
| Publisher Tax ID | GB 494 6272 12 |

Re: Permission to Use Copyrighted Material in a Master's Thesis



Daniel Garry <garry@umn.edu>

8/27/2020 8:32 PM



To: Joanne Muhan Tang

From my standpoint this is acceptable--please get permission from the journal. Good luck, Dan

On Tue, Aug 25, 2020 at 9:51 PM Joanne Muhan Tang [REDACTED] wrote:

Dear Dr. Gary,

I am a Western University graduate student completing my Master's thesis entitled "An approach for the *in-vivo* characterization of brain and heart inflammation in Duchenne Muscular Dystrophy".

I would like permission to allow the inclusion of the following material in my thesis:

- Figure 2: Schematic Diagram of the DGC.

From Kamdar F, Garry DJ. Dystrophin-Deficient Cardiomyopathy. *J Am Coll Cardiol* 2016;67:2533–46.
<https://doi.org/10.1016/j.jacc.2016.02.081>.

Curriculum Vitae

| | |
|---|--|
| Name | Joanne Muhan Tang |
| Post-secondary Education and Degrees | <p>M.Sc. Medical Biophysics candidate (2018-present) Supervisors: Dr. Udunna Anazodo and Dr. Lisa Hoffman <u>Thesis:</u> An approach for <i>in-vivo</i> characterization of brain and heart inflammation in Duchenne Muscular Dystrophy Western University Schulich School of Medicine & Dentistry, London, Canada</p> <p>B. Sc. Honours Specialization in Biology and Major in Medical Science (2013-2018) Western University, London, Canada</p> |
| Honours and Awards | <p>Western Graduate Research Scholarship (2018-2020) \$9000 CDN</p> <p>Child Health Research Day – Second Place Award for Basic Science Oral Presentation (2020) \$200 CDN</p> <p>Canadian Connective Tissue Conference – Best Oral Presentation (2019) \$500 CDN</p> <p>Schulich – Quality of Life Initiative Graduate Research Fellowship (2018-2019) \$8700 CDN</p> <p>Western University – Interdisciplinary Development Initiative in Stem Cell and Regenerative Medicine Summer Studentship (2018) \$3000 CDN</p> <p>Dean’s Honour Roll (2016-2018)</p> <p>Western Scholarship of Excellence (2013) \$2000 CDN</p> |
| Related Work Experience | Graduate Teaching Assistant (2019-2020) Western University |

PUBLICATIONS

Manuscripts Submitted (1):

1. **Tang JM**, McClennan A, Liu L, Hadway J, Ronald J, Hicks JW, Hoffman L, Anazodo UC. *In-vivo* imaging of cardiac and neuroinflammation in Duchenne muscular dystrophy. Submitted to Neuromuscul Disord in August 2020. Under Review. Manuscript ID: NWD-S-20-00539

Manuscript Published (1):

1. **Tang JM**, Jiménez-Padilla Y, Lachance MA, Sinclair BJ. Gut yeasts decrease desiccation survival in *Drosophila melanogaster*. *Journal of Insect Physiology*. 2019;117:103893. <http://dx.doi.org/10.1016/j.jinsphys.2019.103893>

Conference Publications (11):

1. **Tang JM**, McClennan AJ, Hakim S, Hadway J, Smailovic H, Fox M, Anazodo, UC, Hoffman LM. The non-invasive modelling of body-wide inflammation in Duchenne Muscular Dystrophy. 2020 Children's Health Research Day. Abstract – Accepted, Oral Presentation.
2. **Tang JM**, McClennan AJ, Hakim S, Hadway J, Smailovic H, Fox M, Anazodo, UC, Hoffman LM. The non-invasive modelling of body-wide inflammation in Duchenne Muscular Dystrophy. 2020 Canadian Bone and Joint Conference. Abstract –Accepted, Oral Presentation.
3. **Tang JM**, McClennan AJ, Hadway J, Smailovic H, Fox M, Hoffman LM, Anazodo UC. *In-vivo* imaging of inflammatory heart-brain interaction in animal Duchenne Muscular Dystrophy model. 2019 World Molecular Imaging Conference—WMIScan Pre-conference Workshop. Invited Talk.
4. **Tang JM**, McClennan AJ, Hadway J, Smailovic H, Fox M, Hoffman LM, Anazodo UC. *In-vivo* imaging of inflammatory heart-brain interaction in animal Duchenne Muscular Dystrophy model. 2019 World Molecular Imaging Conference. Abstract –Accepted, Oral Presentation.
5. **Tang JM**, McClennan AJ, Hadway J, Smailovic H, Fox M, Anazodo UC, Hoffman LM. Non-invasive modelling of body-wide inflammation in Duchenne Muscular Dystrophy *in-vivo* animal models. 2019 World Molecular Imaging Conference—Late Breaking Abstract –Accepted, Poster Presentation.
6. **Tang JM**, McClennan AJ, Hadway J, Smailovic H, Fox M, Hoffman LM, Anazodo UC. Modelling Inflammatory Heart-Brain Interaction in Duchenne Muscular Dystrophy. 2019 Brain & Brain PET. Abstract –Accepted, Poster Presentation.

7. **Tang JM**, McClennan AJ, Hadway J, Smailovic H, Fox M, Hoffman LM, Anazodo UC. Modelling Inflammatory Heart-Brain Interaction in Duchenne Muscular Dystrophy. *JCBFM* Volume 39 Issue 1_suppl. 2019; PB03-V09. Abstract. Published. DOI: <http://dx.doi.org/https://doi.org/10.1177/0271678X19851020>
8. **Tang JM**, McClennan AJ, Hadway J, Smailovic H, Fox M, Anazodo UC, Hoffman LM. The non-invasive modelling of body-wide inflammation in Duchenne Muscular Dystrophy. 2019 Canadian Connective Tissue Conference. Abstract –Accepted, Oral Presentation.
9. **Tang JM**, McClennan AJ, Hadway J, Smailovic H, Fox M, Anazodo UC, Hoffman LM. Modelling inflammatory brain-heart interaction in Duchenne Muscular Dystrophy. 2019 Child Health Research Day. Abstract –Accepted, Poster Presentation.
10. **Tang JM**, McClennan AJ, Hadway J, Smailovic H, Fox M, Anazodo UC, Hoffman LM. Modelling inflammatory brain-heart interaction in Duchenne Muscular Dystrophy. 2019 London Health Research Day. Abstract –Accepted, Poster Presentation.
11. **Tang JM**, Jiménez-Padilla Y, Lachance MA, Sinclair B. Effects of gut-associated yeasts on *Drosophila melanogaster* water balance. 2018 Ontario Biology Day. Abstract – Accepted, Oral Presentation.